EFFECT OF AGING ON THE TRANSFORMATION OF PHASES IN

SOLDER JOINT OF PBGA PACKAGING

by

JEONG-MIN KIM

Presented to the Faculty of the Graduate School of

The University of Texas at Arlington in Partial Fulfillment of

The Requirements for

The Degree of

MASTER OF SCIENCE IN MATERIAL SCIENCE AND ENGINEERING

THE UNIVERSITY OF TEXAS AT ARLINGTON

December 2009

ACKNOWLEDGEMENTS

This thesis marks the completion of a challenging yet satisfying period in my professional career and it involved the unwavering support of numerous people along the way. To all of them, I would like to express my deepest gratitude and appreciation.

First, special thanks are due to my supervisor, Prof. Choong-Un Kim, for giving chance to study in UTA as well as his continuous support, leadership, guidance and invaluable feedback throughout the entire period of my master course in UTA.

Fruitful and inspiring discussions with my lab members; Dr. Bang, Emil Zin, Lianshan Chen, Huili Xu provided a number of exceptional ideas and helped stimulate and motivate me in my endeavor. Also, the contributions of Dr. Jiang and Dr. Yan at the CCMB are gratefully acknowledged.

I would like to express my sincere gratitude to Prof. Je-Hyun Lee in Changwon National University for not only giving me chance to study abroad but also his constant encouragement and boundless support.

I would like to thank my committee members Dr. Goolsby and Dr. Aswath for their time to review my thesis and for their valuable suggestions.

In addition, I wish to thank Bo-Hoon Kim, Soo Kim and TJ Adeogba for their continuous consideration and support, especially at times when I needed the most.

Finally, I thank my parents, my younger brother and my lover, Ga-Young for their endless understanding throughout the course of this master course and ceaselessly supporting me in a myriad of ways, from offering encouragement to providing love and praise.

December 7, 2009

ABSTRACT

EFFECT OF AGING ON THE TRANSFORMATION OF PHASES IN

SOLDER JOINT OF PBGA PACKAGING

Jeong-Min Kim, M.S.

The University of Texas at Arlington, 2009

Supervising Professor: Choong-Un Kim

This study investigates the microstructural characteristics of 3.0Ag-0.5Cu-Sn (SAC305) solder joint as in assembled state, and their evolution with aging treatment at 100 and 150°C for various hours. Specific aim of the study is 1) to understand thermodynamic stability of as-reflowed microstructure (β-Sn dendrite, inner dendrite Cu_6Sn_5 intermetallic (IMC) compound, and the eutectic structure), 2) to find direction of their change with aging, and 3) to relate interfacial reaction to such evolution in microstructures. This investigation is spurred by the findings made in a separate study where fatigue resistance of solder joint and failure location shows markedly keen dependence on aging treatment of the joint. The findings made in the present investigation reveals supporting evidences that the change in fatigue reliability is closely related to the change of mechanical properties induced by evolution of microstructure that are not uniform within solder matrix and interfaces.

There are three main findings made in this investigation bearing scientific and engineering importance. The first is the fact that the as-reflowed SAC305 solder joint

undergoes non-equilibrium solidification due to rapid cooling during solder assembly and large super-cooling of β-Sn, resulting in a larger fraction of unstable β-Sn dendrite than equilibrium and near binary Ag_3Sn-Sn eutectic (not ternary eutectic). This, non-equilibrium solidification, results in solder microstructure that is thermodynamically unstable. Therefore, several unusual changes are found to occur by aging treatment. Among many, the most remarkable change is the disappearance of Cu-rich phase from the eutectic pool. It is believed that such a change is resulted because the eutectic formed at as-reflowed state is not true ternary eutectic (due to consumption of Cu by growing Sn-dendrite). Coarsening of Ag_3Sn and Sn phases within eutectic pool is observed. Also found is the fact that β-Sn dendrite collapse with aging, growing to one grain. This result, coarsened Sn grain structure, is especially note-worthy because it may be one of the main sources that reduce the fatigue reliability with aging.

The second finding made in this investigation is the fact that as-reflowed SAC 305 is enriched with Cu due to entrance of Cu from Cu pad during interfacial reaction at reflow temperature. The addition of Cu is found to be sufficient amount to change the solidification sequence of the alloy. Specifically, bulk alloy of SAC305 is known to show solidification sequence of β-Sn, Ag_3Sn and finally ternary eutectic. In the current case, it is found that the alloy solidifies with sequence of Cu_3Sn, β-Sn and eutectic. The enrichment of Cu is especially significant at the interface between solder and Cu pad, probably because Cu pad acts as a source of Cu.

The third finding is related to the growth of inner dendrite Cu_6Sn_5 IMC. It is found that aging treatment makes solder to be continuously enriched with Cu through solid state diffusion of Cu through Cu/solder interface. On the other hard, the Cu enrichment, seen as increase in Cu_6Sn_5 volume fraction, at Ni interface side is found to be minimal or even absent. This result suggests that the solder near at Cu pad interface would continuously strengthened with Cu addition (precipitation hardening), while such strengthening is absent in the solder near at Ni interface. This may explain the fatigue failure location change with aging, which is found to

occur initially at Cu/solder interface (due to a large strain singularity) but change to Ni/solder interface after aging treatment.

　　While more study is necessary in order to better understand the unique metallurgical mechanisms of microstructural evolution found in the present study, the results and understanding gained so far provide sufficient evidence that conventional approach to solder reliability assessment, which is based largely on interface IMC microstructure, needs to be changed.

TABLE OF CONTENTS

viii

LIST OF ILLUSTRATIONS

LIST OF TABLES

CHAPTER 1

INTRODUCTION

1.1 Packaging

The electronics industry is one of the most fascinating, dynamic, and important industries. It has literally transformed the world and provides many products that affect our daily lives- for example, telephone, television, high-definition television, electronic organizers, personal computers, notebook PCs, subnotebook PCs, laptop PCs, palmtop PCs, PCs with built-in portable phones, workstations, midrange, mainframe, and supercomputers, PC cards, cellular phone, wireless phones, pagers, portable electronics products, video camcorders, audiovisual products, military equipment, aerospace part, etc. One of the key technologies that is helping to make these products possible is electronics packaging and assembly technology.

Electronic packaging is to make a certain structure, including a semiconductor chip, which can be mounted on components like PCB (printed circuit board) for actual usage. In order to establish this type of structure, there are various considered factors. Therefore, an electronic package is designed to protect an Integrated Circuit (IC) from electrical, mechanical, chemical, and thermal harm while providing interconnections to other devices. This function becomes increasingly difficult as ICs become increasingly more complex in order to meet the self-fulfilling prophecy of Moore's Law [1, 2], which in one interpretation states that the transistor density on an IC will double every 18 months [3]. The increase in transistor density relates to an increase in the number of interconnections coming form the chip to the substrate of printed wiring board (PWB).

Electronic packages contain hundreds to millions of transistors on a silicon chip in addition to many discrete components such as resistors, inductors and capacitors. All these different transistors and discrete components should be connected to each other and suitably

powered to ensure optimal functionality and speed. With the technology increasingly being moved to the silicon chip level, protection of the silicon chip from outside environment and from shock and vibration is necessary. Increased functionality and increased power consumption also causes the electronic package to overheat. The package should be designed so as to provide adequate means for thermal heat dissipation and cooling. Thus electronic packaging has four main functions [4]:

- Signal distribution which involves topological and electromagnetic consideration.
- Power distribution, involving electromagnetic, structural and material consideration.
- Heat dissipation, involving structural and materials consideration.
- Mechanical, chemical and electromagnetic protection of components and interconnections.

1.2 Evolution of Electronic Package

All technologies from the silicon chip level to the printed wiring board level collectively belong to the packaging hierarchy. A schematic of the packaging evolution from early 1970s to today is given in Figure 1.1 and Figure 1.2. Dual In-Line package (DIP) was the initial packaging technology started in the 1970s. In a DIP, the Input/Output (I/O) connections in the form of pins are arranged along the periphery of the package. The DIP had a very low silicon efficiency of about 2%. Silicon efficiency is defined as the percentage of the functional Printed Circuit Board (PCB) area taken by the silicon. The packaging technology has evolved significantly since then to meet the demands of higher signal speed, smaller package size, increased functionality for a given area and lower cost. To achieve higher I/O connection per package, the peripheral array evolved into an area array package known as Pin Grid Array (PGA) package. The Small Outline Package (SOP) was developed because of the cost benefits it offered. This later evolved into Quad Flat Packs (QFP) which allowed greater I/O connections per package.

2
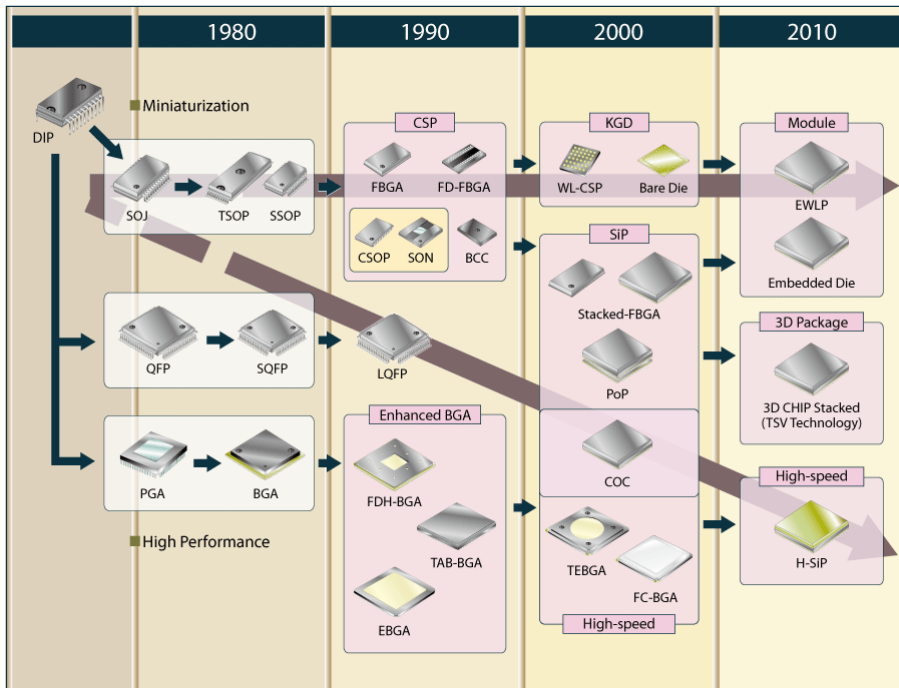
Figure 1.1 Evolution of electronic packaging technology [Courtesy: FUSITSU®]
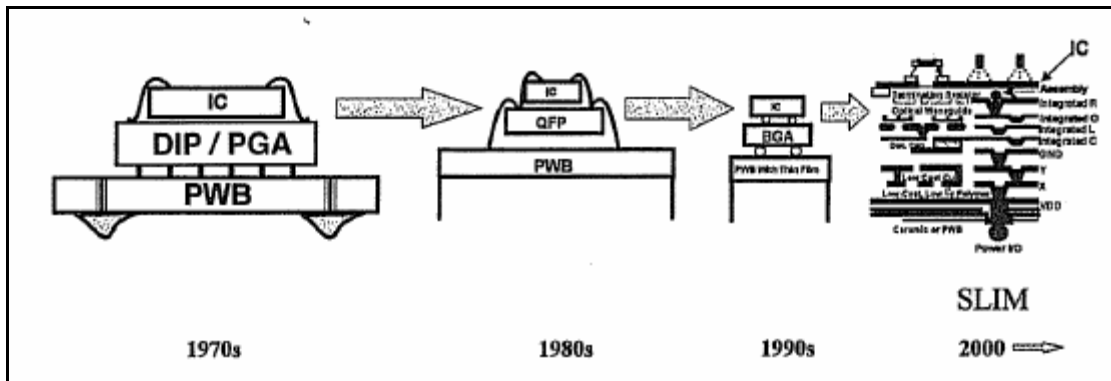
Figure 1.2 General evolution of electronic packaging technology [4]

3

All the packages mentioned above are through-hole packages which require drilling a hole in the PCB to assemble the packages. Through-hole packages leave significant amount of area on the back side of the board unutilized. Surface mount alternatives to these packages were developed in the 1980s. Surface mount packages, also known as Ball Grid Array (BGA) packages, used solder joints instead of pins to assemble the packages on the board. In addition to making available an increased board surface area for additional components placement, the solder joints also reduces the electrical parasitics significantly due to their smaller interconnect lengths. BGA packages have smaller form factors compared to through-hole packages. The BGA packages evolved further in the 1990s to Chip Scale Package (CSP). In a CSP, a package size to silicon size ratio of 1.2 can be achieved.

BGAs and CSPs satisfy most of the requirements of today's microelectronic industry's demands. A large number of variations exist within BGA and CSP package types. To name a few, the variations are based on the type of material used for the package substrate, the number of silicon chips in the package and the manner by which the silicon chips are assembled on the package substrate.

The BGA and CSP packages have evolved into Flip Chip On Board (FCOB) packages where the silicon chip is directly placed on the board. This reduces the number of levels in the packaging hierarchy to one, thereby increasing the signal speed significantly. However, increased difference in the thermal expansion coefficient between the silicon chip and the board leads to large number of reliability issues. Design considerations also require additional precaution to protect the silicon form outside environment.

Current state-of-the art in packaging technology is a single level integrated module (SLIM) as shown in Figure 1.2. This method allows inclusion of the silicon chips and discrete components into one single level module. Due to shorter interconnect lengths higher signal speed can be achieved compared to any surface mount package. BGA packages allow only placement of finite number of discrete components inside the package. The remaining discrete

components have to be placed on the PCB. BGA packages can therefore achieve a silicon efficiency of only about 25%. SLIM, on the other hand, has the capability of achieving up to 75% of silicon efficiency. The SLIM technology is however still in the research stage.

<u>1.3 Plastic Ball Grid Array Package</u>

A BGA package is a method of reducing package size and pin-to-pin trace gap in order to integrate more functions and reliability in a single space. The BGA package construction is different from conventional leaded packages in several ways. A BGA typically uses a BT-resin based organic substrate (similar to Printed Circuit Board) for die and wire attachment. This substrate incorporates metallized trace routing for connection of the die to the system board through solder balls, instead of metal leads used in leaded packages. Figure 1.3 shows the BGA Package. However, BGA packages also have several common features with the conventional leaded packages. These include similar chip level assembly techniques for die attach, wire bond, and over molding. BGA packages also use conventional test, packing, handling, and PC board assembly methods.

BGAs offer several distinct advantages over fine pitch surface mount components having gull wing leads, including the following:

- High pin count capability, generally more than 200, but gull-wing leads are often limited to less than 300 I/Os;

- Larger lead pitches, which significantly reduces the manufacturing complexities for high I/O parts;

- Higher packaging densities are achievable since the lead envelope for the gull wing leads is not applicable in the case of BGAs; hence, it is possible to mount more packages per board, i.e., higher packaging density;

- Faster circuitry speed than gull wing SMCs (surface mount components) because the terminations are much shorter and therefore less inductive and resistive;

- Better heat dissipation;

5

• Conventional SMT production technologies such as stencil printing and component
mounting can be employed.

The BGAs are also robust in processing. This stems from their higher pitch (1.27 mm,
0.050", typical), better lead rigidity, and self-alignment characteristics during reflow processing.
This latter feature, self-alignment during reflow (attachment by heat), is very beneficial and
considerably opens the process window.

However, there are some drawbacks as well. BGAs are not compatible with multiple
solder processing methods like wave soldering, and individual solder joints cannot be inspected
and reworked using conventional methods. In ultra low volume SMT assembly applications, the
ability to visually inspect the solder joints has been a standard inspection requirement and is a
key factor for providing confidence in the solder joint reliability. Advanced inspection techniques,
including X-ray, need to be used to provide such confidence for BGA and Flip Chip Ball Grid
Arrays (FCBGA).

The chief drawbacks of both BGAs and FCBGAs are similar. These are as follows:

- Lack of direct visual inspectability;

- Lack of individual solder joint reworkability;

- Interconnect routing between the chip and the PWB necessitates a multilayer PWB;

- Reduced resistance to thermal cycling due to use of rigid balls/columns in BGA
packages;

BGA packages truly reflect the advantages and disadvantages of area array
interconnection mentioned above.

A three dimensional view giving the schematic of a PBGA package is shown in Figure
1.4. Bimaleimide Triazene (BT), polyimide and flame retardant fiber reinforced epoxy (FR4) are
commonly used substrate materials in a PBGA package. The silicon chip is attached to the
substrate using an epoxy based die attach material. The I/O pads on the chip are wire bonded
to the I/O pads on top of the substrate. The chip and the wire bonds are encapsulated with a

6

polymer mold compound. The mold compound protects the wire bonds and the silicon chip from moisture, ionic contaminants and hostile operating conditions such as vibrations and mechanical shock loadings. I/O pads on top of the substrate are routed out to I/O pads on the bottom of the substrate through multilayered copper traces and vias within the substrate. The I/Os on the bottom of the substrate are solder bumped thereby allowing the package to be reflowed and assembled onto a PCB.

PBGA packages are typically used for Static Random Access Memory (SRAM) applications, Application Specific Integrated Circuits (ASICs) and lower frequency microprocessors. The self aligning ability of ball grid array (BGA) packages ensures a very high yield with defect rates less than 1 ppm on a per-joint basis.
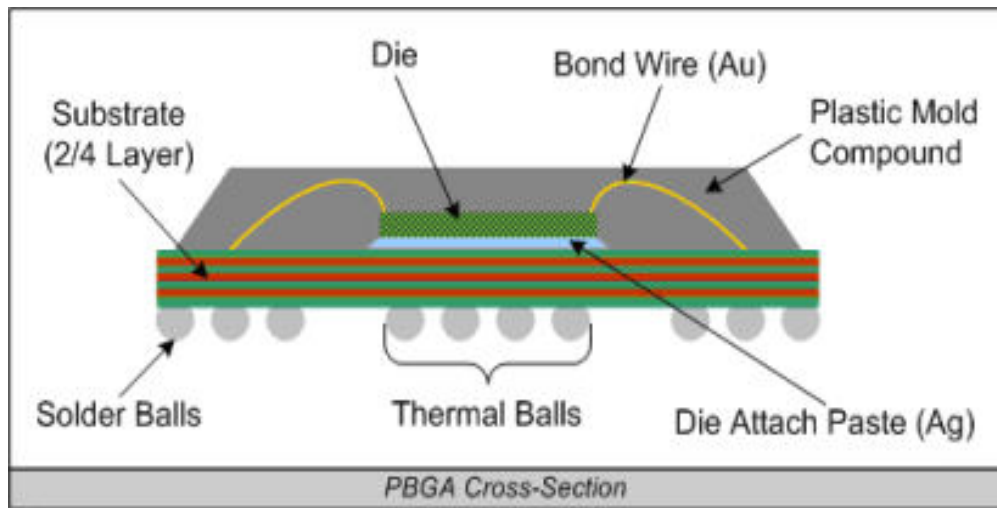
Figure 1.3 Schematic of a wire-bonded face-up silicon chip PBGA [Courtesy: TOSHIBA®]
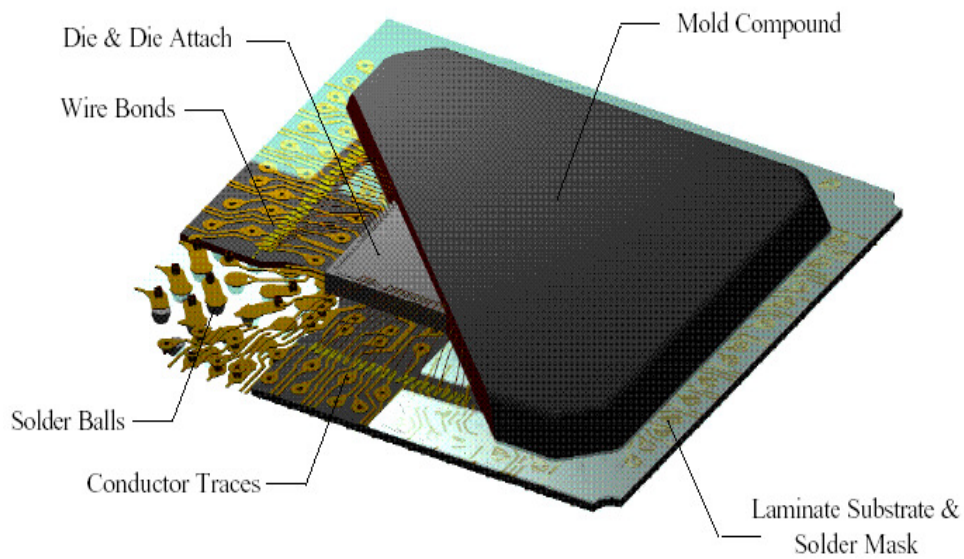
Figure 1.4 Plastic ball grid array package [Courtesy: ChipPAC incorporated]

<u>1.4 Lead-Free Solder</u>

The solder joints provide electrical connection between the BGA package and PCB and also provide mechanical support to the package. Tin-lead based solders have been used for the past few decades due to their low melting point and good mechanical properties. However, over the past few years, legislations in Europe and Japan have been passed banning the use of lead in any solder alloys due to potential environmental and health concerns. The European Commission's (EC) draft directive, Waste Electrical and Electronic Equipment (WEEE) and Restriction of Hazardous Substances (ROHS) have proposed the ban on lead in electronics by the 1st of July 2006. Legislation for banning lead in United States was proposed in 1989 but was dropped due to the then existing small lead consumption by electronic industries and due to increased pressure from the electronic industry to retain lead based solders. The need for the alternative to lead-free electronics in United States is therefore now driven by market competition. It is not possible to sell leaded products in Europe or Japan or in any country where the use of lead based products is prohibited. The adaptation to lead-free electronics therefore seems inevitable.

A consortium conducted by National Center for Manufacturing Sciences (NCMS) concluded that there is no drop-in replacement to lead-based alloys [5]. Sn based solder alloys with minor additions of Ag, Cu, Bi and Zn have been recommended by National Electronics Manufacturing Initiative (NEMI) and Japan Electronic Industry Development Association (JEIDA). Prominent among them were the Sn-Ag alloy for the wave soldering process and Sn-Ag-Cu (SAC) based solder alloy for reflow soldering process. NEMI has recommended Sn4.0Ag0.5Cu (SAC405) alloy [6] and JEIDA has recommended Sn3.0Ag0.5Cu (SAC305) for reflow soldering process [7]. SAC405 and SAC305 based alloys will be the focus of the present research.

Tin-lead solders have been used for the past few decades and their mechanical behavior is very well understood. Extensive legacy data related to their deformation behavior

9

during thermo-mechanical loading is available. SAC alloy on the other hand is a relatively new alloy having about 35℃ higher melting point compar ed to eutectic Sn-Pb solders [8]. The microstructure and mechanical behavior of SAC alloy is known to be very different from lead-based alloys. The microstructure of a typical Sn-Pb solder joint is poly-crystalline and consists of a uniform distribution of tin-rich and a lead-rich phase [9]. SAC based solder joints however have very few grains per solder joint (typically one to ten) [10] and can be described as multi-crystalline. Sn has an orthogonal body centered cubic (BCC) lattice and therefore has an orthotropic coefficient of thermal expansion (CTE) and modulus [11-13]. With very few grains present in a solder joint, the mechanical behavior of a solder joint is expected to be not homogeneous. These Sn grains are made up of colonies of β-Sn dendrites and Sn-Ag-Cu eutectic. The Sn-Ag-Cu eutectic regions contain Ag_3Sn and Cu_6Sn_5 precipitates which offer resistance to creep deformation at low stresses [14]. At high stresses however, these precipitates do not seem to be effective enough and the creep deformation rate is known to be higher than that for eutectic Sn-Pb solder [14].

1.5 Solder Joint Reliability of Semiconductor Package

Except for a few application, Pb-free alloy replace the Sn-Pb alloy as a solder material in most of case. In the transition from traditional Sn-Pb materials to Pb-free materials, one of the largest concerns is the impact on solder joint reliability. While the integrity of Sn-Pb solder joint is backed by decades of experience and an abundance of empirical data, relatively less is known about Pb-free solder joint. Further, there are a number of different alternatives in PCB finish, component plating, and solder alloy used in assembly. It is critical, therefore, that the electronics assembler understands the metals comprising the final solder joint and the resulting microstructure. Of particular importance is the type and amount of intermetallic formation at the interfaces between the bulk solder and the component, between the bulk solder and the PCB substrate, and within the bulk solder itself. Intermetallic formation at the interface is necessary to form a solder joint, and intermetallic compound structures within the bulk solder can actually

10

serve to strengthen the solder joint by resisting crack propagation. However, in excessive amounts or thickness, these compounds can contribute to brittle fracture of the solder joint from cyclic shear stresses and strains imposed by temperature and/or power fluctuations experienced in the field.

Semiconductor packages are exposed to various environments, such as temperature, humidity, dust, shock and vibration, which contribute to failures as shown in Figure 1.5 [15]. Temperature is the major cause of failure by inducing thermal stress in the solder joints under normal operating conditions due to the differences in the coefficients-of-thermal expansion (CTE) between the chip and board. Currently, accelerated thermal cycling (ATC) tests are run to evaluate solder joint reliability, to minimize time-to-market, and to satisfy customer expectation of long term reliability by inducing thermal stress levels higher than those experienced in normal operating conditions.
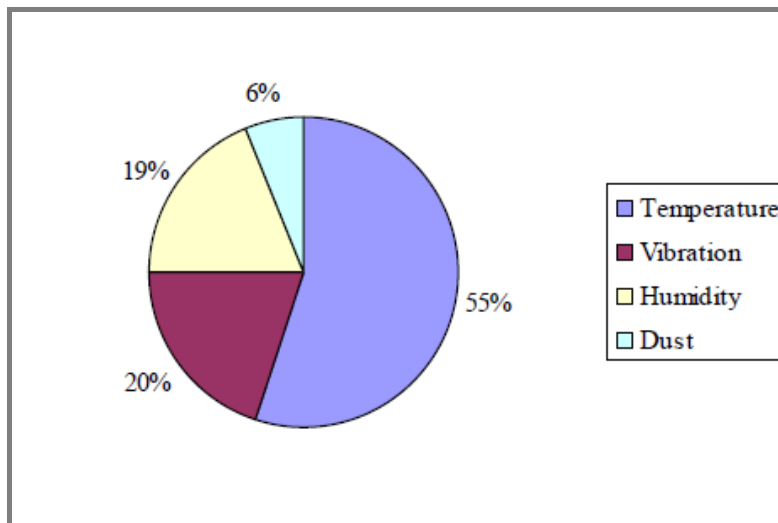
Figure 1.5. Causes of failures in electronic packages [15]

1.6 Objectives of This Research

As mentioned above, PBGA packaging consists of various materials, including Pb-free solder and polymer, etc., and used for a variety of application in various environments. Therefore, the reliability of PBGA packaging has been being one of hot issues for electronic industry. Hence, nowadays numerous researches related to reliability problems are ongoing. From these researches, the failure mechanisms of applications used at high homologous temperature condition have been being disclosed. The mechanisms mentioned from those researches are creep, thermal fatigue, IMC formation/growth and constitutive factor, etc.

Our research group also has been performing research related to packaging reliability. Our recent study finds that the solder joint failure is not uniquely defined in a specific place, as commonly reported in other literatures, but changes with aging condition and thus microstructural variation of solder joint. Specifically, our bending fatigue test shows that cracking occurs at solder-metallization interface at as-received condition, while the location for cracking moves to interior of intermetallic compound and to solder itself with progression of solder aging. It is clear that this transition in failure location is resulted by the change in solder joint microstructure with aging, yet the exact microstructural change responsible such variation is not fully understood. This objective of this thesis therefore aims to track the change in the joint microstructure and identify the source of metallurgical process leading to the observed property changes in the solder joint.

Specifically, this thesis demonstrates that

- As-solidified lead-free solder may have a non-equilibrium microstructure due to rapid cooling. More specifically, the non-equilibrium cooling may promote the development of microstructure that consists of primary Sn and Ag-Sn binary eutectic rather than the Sn-Ag-Cu ternary eutectic microstructure. Aging, that drives the microstructure toward an equilibrium structure, induces evolution of

12

microstructure that can be explained only by the presence of primary Sn and Ag-Sn binary eutectic.

- Bulk microstructure of lead-free solder and mechanical properties are found to vary significantly with aging because aging makes Cu to enter the solder through reaction and diffusion. However, the enrichment of Cu is found to show disparity between Cu/solder interface and Ni/solder interface. It is found that Cu/solder interface acts as Cu source and Ni/solder interface as its sink, leading to enrichment of Cu in area closer to Cu metallization while little variation is seen at Ni/solder interface.

1.7 Thesis overview

This thesis is organized into five chapters. The first chapter is essentially an introduction to this research, providing the research objective along with a brief description of each chapter. A comprehensive review of literature was conducted and is summarized in the second chapter. Literature in Chapter 2 was reviewed on SAC lead free solder alloys, surface finishing method and solder microstructure evolution affected by various factors.

The third chapter discusses the experimental strategy adopted and the design of experiment used for the research. The fourth chapter discusses the results of the experiments and analysis the results. The fifth chapter concludes the research based on the observations made during the research.

CHAPTER 2

BACKGROUND AND LITERATURE REVIEW

2.1 SAC Solder Alloy

2.1.1. Advent of SAC Solder Alloy for Packaging Industry

To be considered an alternative to Sn-Pb solder, lead-free candidates should have similar or better properties and reliability to those possessed by eutectic or near eutectic Sn-Pb solders. According to recent reports [16, 17], Pb in solders contributes outstanding properties to the overall reliability of the Sn-Pb solder, such as the following:

- Pb reduces the surface tension of pure tin to improve the wetting ability.

- Pb enables tin and copper to rapidly form intermetallic compounds by diffusion.

- Pb provides ductility to Sn-Pb solders.

- The addition of Pb prevents the transformation of β-tin to α-tin. If the transformation occurs, it will cause dramatic volume increase and loss of structural integrity and hence a loss of reliability. The β-tin to α-tin transformation in lead-free solders is also called "tin pest" or "tin disease". Karlya et al. observed significant "tin pest" phenomena in their lead-free solder specimens [18].

- Sn-Pb solders have a low melting temperature of 183 °C for eutectic solder, which allows the use of a low reflow temperature in the electronic packaging process and ensures the reliability of the packages.

Besides all of the above benefits of Pb, the cost of Pb is also low and it is very abundant. However, Pb is toxic, which causes the pressure from legislations worldwide.

Lee proposed some basic criteria for "perfect" lead-free alternatives [19]. The lead-free solder needs to have a similar melting temperature to existing Sn-Pb solders, particularly

14

eutectic and near eutectic solders, in order have a similar reflow profile during the manufacturing process; good wetting ability to ensure good metallization in the manufacturing process; the same or better electrical properties to efficiently transmit the electrical signals; and adequate mechanical properties, such as creep, and fatigue, etc. to preserve the reliability of the electronic packaging products. The new lead-free solders also need to be non-toxic and relatively inexpensive.

A considerable amount of research is currently underway in the lead-free solder area, including projects organized by consortia including the HDPUG (High Density Packaging Users Group), the National Center for Manufacturing Sciences (NCMS), the National Institute for Standard and Technology (NIST), the National Electronics Initiative (NEMI), and the Japan Electronic Industry Development Association (JEDIA). Although no "drop in" replacement has been identified that is suitable for all applications, Sn-Ag, Sn-Ag-Cu (SAC), and other alloys involving elements such as Sn, Ag, Cu, Bi, In, and Zn have been identified as promising replacements for standard 63Sn-37Pb eutectic solder. Several SAC alloys have been proposed by industrial consortiums. These include 96.5Sn-3.0Ag-0.5Cu (SAC 305) in Japan, 95.5Sn-3.8Ag-0.7Cu (SAC 387) in the EU, and 95.5Sn-3.9Ag-0.6Cu (SAC 396) in the USA. In addition, 95.5Sn-4.0Ag-0.5Cu (SAC405) has been widely adopted as an alloy for use in BGA solder joints. The main benefits of the various SAC alloy systems are their relatively low melting temperatures compared with the 96.5Sn–3.5Ag binary eutectic alloy, as well as their superior mechanical and solderability properties when compared to other lead-free solders. A survey conducted by Soldertec shows approximately 70% of the market for reflowing lead-free solders are in the SAC series (Figure 2.1) [20]. There are some major challenges for the current series of lead-free solders. SAC series alloys have a higher melting temperature, around 217 ℃, compared to 183 ℃ for the eutectic Sn-Pb solders. They thus require higher reflow temperature during the manufacturing process, which lead to reliability problems. The excessive build up of intermetallics formed at the interface between the solder joints and the copper pad can cause

15

reliability problems. Regardless all of these problems, the SAC series lead-free solders have been widely accepted by both industry and academic institutions. However, unless a "perfect" lead-free solder is found to replace the Sn-Pb series solders, research into new lead-free solders will continue for years to come.
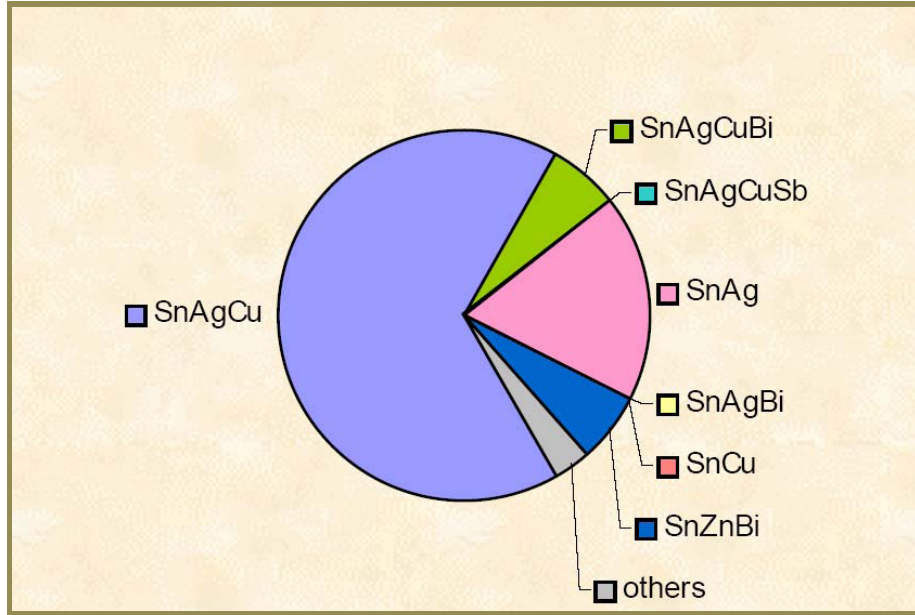
Figure 2.1 The Market Share of Different Lead-free Solders [20].

2.1.2. Sn-Ag-Cu Lead-Free Solders Series

Of the many lead-free solder series proposed in the last decade or so, Sn-Ag-Cu (SAC) series alloys have emerged as the most widely accepted (Figure 2.1). Soldertec's survey shows that the most popular SAC are the near eutectic SAC alloys [20], which consist of 3.0-4.0% of Ag and 0.5-1.0% of Copper (Figure 2.2). The melting point of these near eutectic SAC alloys is around 217°C, which is lower than the 96.5Sn–3.5Ag binary eutectic alloy at 221 °C. In the SAC system, the addition of Cu both lowers the melting temperature and improves the wettability [21]. Figure 2.3 shows a typical 3-D ternary phase diagram [22]. The contours on the top surfaces of the figure represent the isothermal lines. Each of the 3 sectors represents the binary phase

16

diagram of two of the three elements. The center of the diagram, where the isothermal lines reach the common, lowest point, is the eutectic point of the ternary system [23]. Figure 2.4 is the top view (2-D) of the ternary phase diagram of Sn-Ag-Cu. The area indicated in the red box is the near eutectic region. Most of the SAC alloy compositions currently on the market are within this region. The eutectic and near eutectic melting temperature has been determined to be 217 ℃, although the precise eutectic point is n ot known [21].

In SAC alloys, the formation of intermetallic compounds between the primary elements Sn and Ag, and Cu affect all the properties of the alloys. According to the binary phase diagram shown in Figures 2.5-2.7, there are three possible intermetallic compounds that may be formed: Ag_3Sn forms due to the reaction between Sn and Ag (Figure 2.5) and Cu_6Sn_5 forms due to the Sn and Cu reaction (Figure 2.6), but Cu_3Sn will not form at the eutectic point unless the Cu content is high enough for the formation of Cu_3Sn at higher temperatures, so in bulk specimens Cu_3Sn is not presented. Ag can also react with Cu to form Ag rich α phase and Cu rich β phase (Figure 2.7). However, there is no reaction between Ag and Cu to form any kind of intermetallic compounds. Figure 2.8 shows a typical SAC structure with eutectic Sn matrix (2 in the picture) with Ag_3Sn (1 in the picture) intermetallic compounds [24]. The particles of intermetallic compounds possess much higher strength than the bulk material [25, 26]. Fine intermetallic particles in the Sn matrix can therefore strengthen the alloys. The intermetallic compounds can also improve the fatigue life of the solders, as SAC alloys are reported to be 3-4 times better fatigue properties than the Sn-Pb eutectic solders [27]. The higher fatigue resistance is believed to be contributed by the interspersed Ag_3Sn and Cu_6Sn_5 particles, which pin and block the movement of dislocations [27]. The many patents that have been granted for SAC systems have limited their use and hindered research on several of the SAC alloys, but fortunately the alloy Sn-4.0Ag-0.5Cu has not been patented [28].
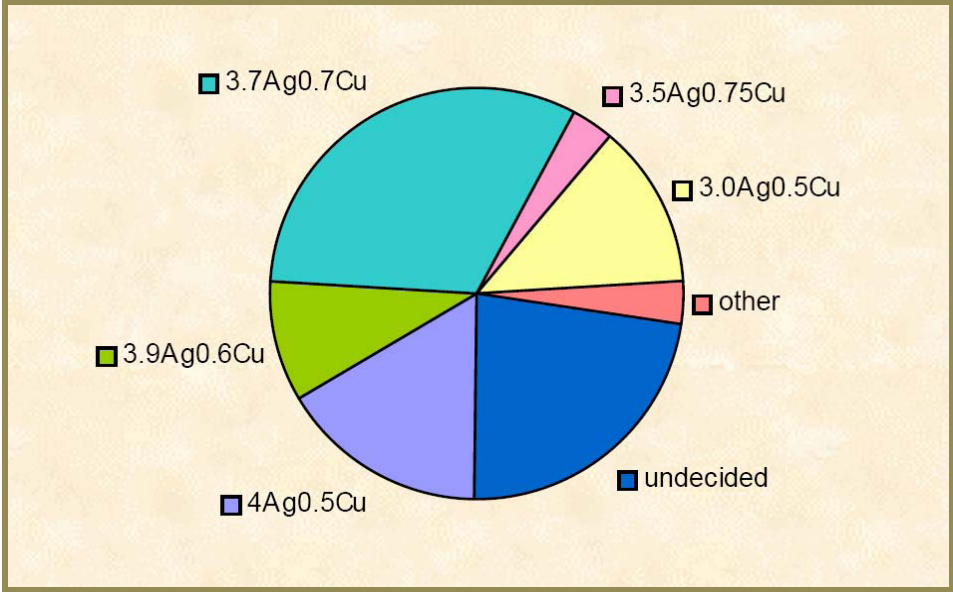
Figure 2.2 Survey of the Market Share of Different Types of SAC Alloys [20].
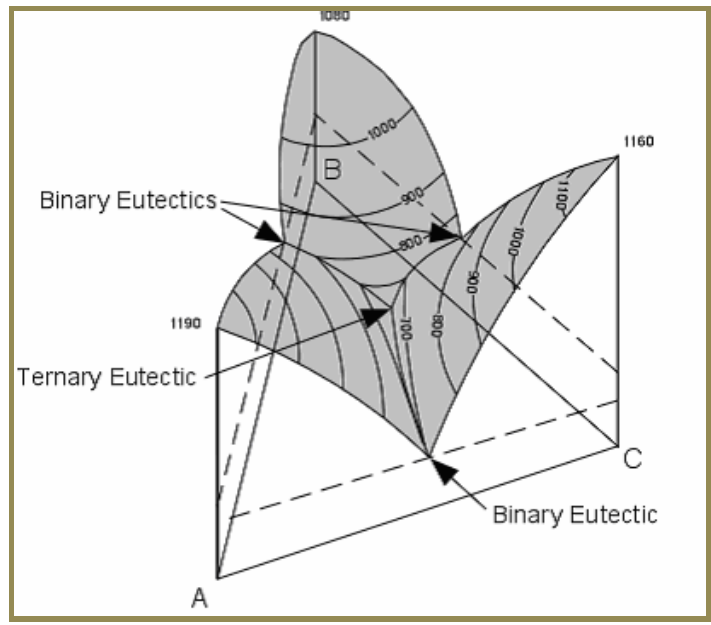
Figure 2.3 Typical 3-D Ternary Phase Diagram [22].
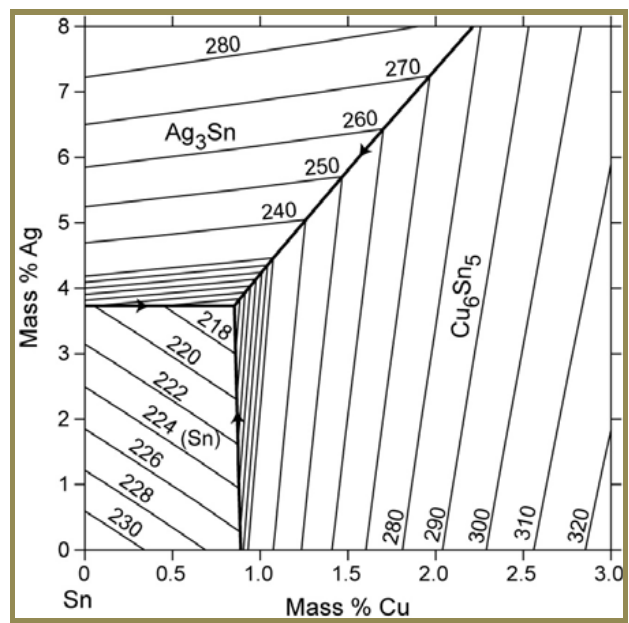
Figure 2.4 Sn-Ag-Cu Ternary Phase Diagram [23].

19
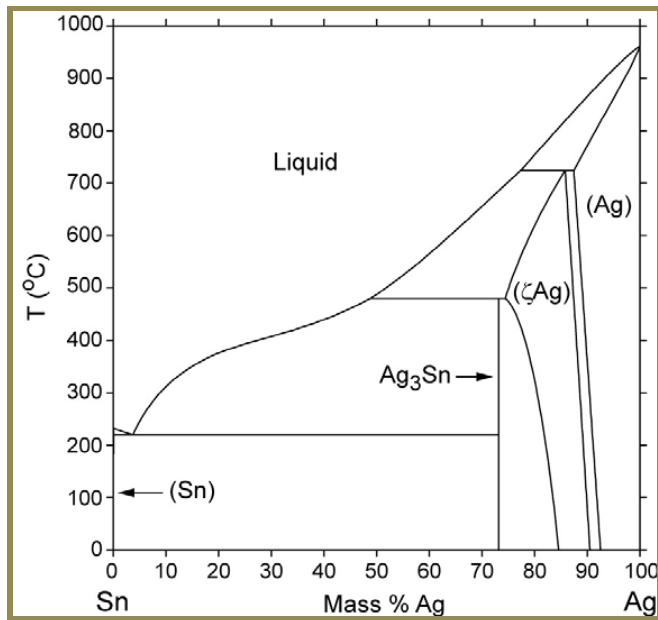
Figure 2.5 Sn-Ag Binary Phase Diagram [23].
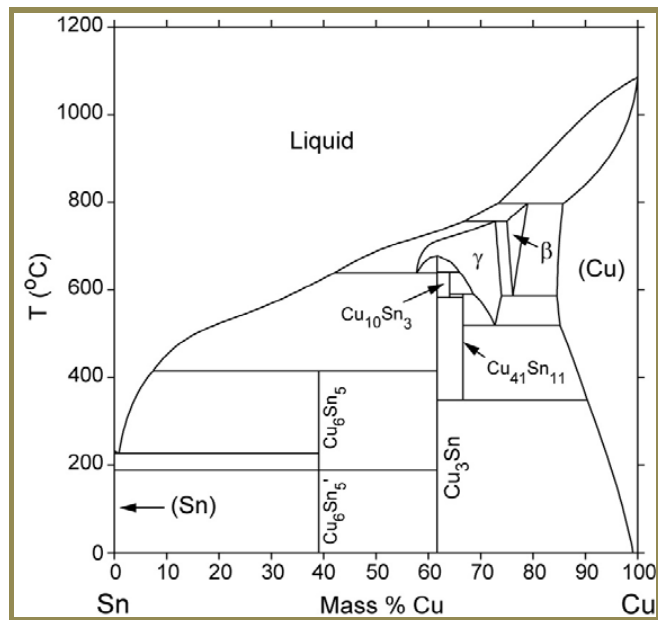
Figure 2.6 Sn-Cu Binary Phase Diagram [23].
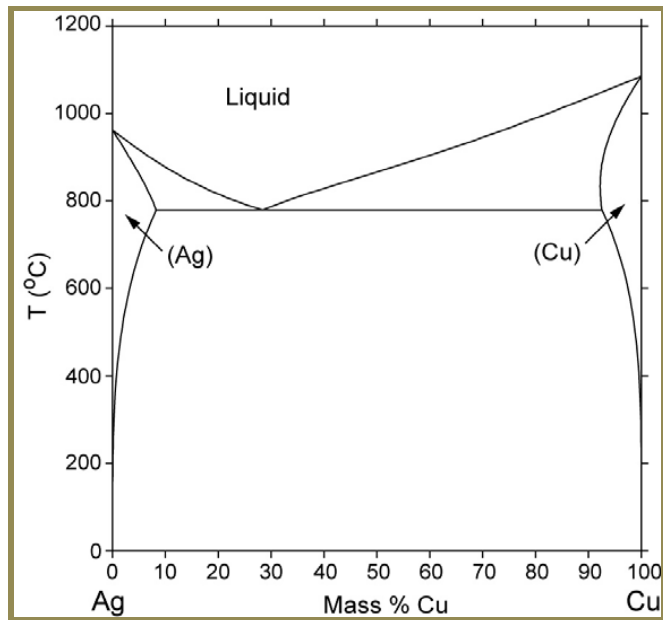
Figure 2.7 Ag-Cu Binary Phase Diagram [23].
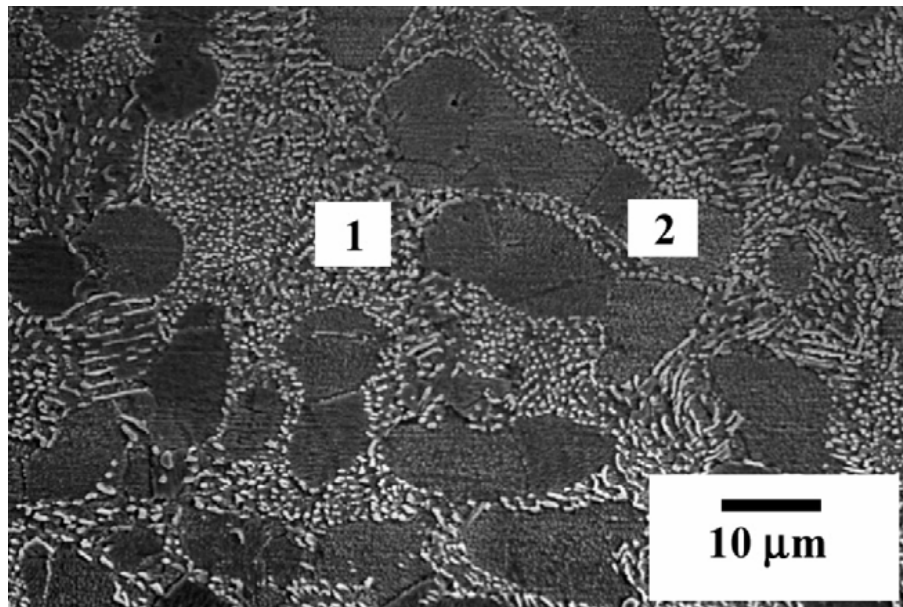
Figure 2.8 Typical Microstructure of SAC Alloys [24].

<u>2.2 Surface Finishes for Solder Pad</u>

Copper is the most commonly used base material for solder pads on printed circuit boards. Alloys with high tin content and high melting point have a tendency to dissolve copper. If an excessive amount of copper gets dissolved in the solder material, then it leads to the formation of the Cu_6Sn_5 intermetallic layer. This intermetallic layer is extremely brittle. Reliability of the solder joint can be affected by the brittle nature of this compound [30]. Hence, some kind of surface finish is required to prevent the diffusion of copper. Because it is important to protect the copper on PCBs from degradation, PCBs are applied with finishes using different surface finish options as discussed below. Because a fully leadfree electronic assembly will call for there to be no lead in the finish, board fabricators must select an alternative rated on cost, reliability, and shelf life.

Many Pb-free surface finishes are available for printed circuit boards. Surface finishes such as Ni-Au and OSP have a long history of usage. A list of available surface finish options are shown below:

- OSP – such as benzotriazole or benzinidazole
- Immersion silver (Ag);
- Immersion Au/Electroless Ni;
- HASL(Sn/Cu)
- Sn/Bi
- Electroless Pd/Electroless Ni
- Elecroless Pd/Cu
- Elecroless Ni/Au

2.2.1 Organic Solder Protectants (OSPs)

OSPs are a viable candidate because they are almost in the same price range as Sn/Pb but contain no lead. These finishes can also be easily processed, are relatively free of

22

ionic contaminants, and are smoother than HASL. They also have good solderability (based on solder atmosphere selection) and are re-workable. These finishes are known for their short storage life, which can be up to 12 months if stored properly (i.e., dry nitrogen, desiccants), but manufacturers with quick turnover of PCBs may not see this as an issue. There are also concerns with handling of these finishes, durability with higher soldering temperatures, and flux used. With lead-free alloys, however, they do not seem to wet as well as other finishes. Theoretically, if an oxide-free surface can be obtained with a thin layer of organic coating, flux penetration and the overall solderability should improve. However, most thin coatings have limited ability to protect the copper from oxidation. Research efforts have been performed to produce thinner coatings while maintaining the robustness of the OSP. It has been shown by Stafstrom et al. [31] that the initial organo-copper layer and the structure of the OSP are key to the thinner coating's ability to limit oxidation. It has been demonstrated that a no-clean soldering of a standard OSP yields excellent results with thinner coatings. If reflowed in nitrogen atmosphere, a high percentage of coating is removed, leaving a thinner oxide-free surface for improved solder wetting.

2.2.2 Lead-free Hot Air Solder Level (HASL)

Even though lead-free HASL is available for PCBs, some manufacturers may choose to move away from this process if required to produce a lead-free product. Even though close to 70% of the PCBs currently produced worldwide are thought to be HASL finished, problems such as flatness of the finish make it difficult to mount small components or components, such as QFPs with fine pitch [32]. If chosen, alternative HASL finishes will most likely work well with most alternative alloys and will wet faster than plated finishes or coatings. Concerns with this finish include warpage due to higher processing temperatures and PCB absorbed process chemistries, although they can sometimes be removed with cleaning.

2.2.3 Immersion Finishes

Immersion finishes have been considered as replacement for HASL because of their surface flatness and ease of processing. There are some concerns regarding the thinness of the coating, because higher soldering temperatures could result in out-diffusion of base metals and oxidation, leading to reduced solderability.

Among the immersion finishes, Immersion Silver and Immersion Tin are already being used and also studied to encounter their compatibility with lead-free alloys. Tin whisker is considered to be a major roadblock in consideration of Immersion Tin.

2.2.4 Electroless Ni-Au (Electroless Nickel Immersion Gold)

These finishes are attractive because of their resistance to damage during handling/processing and improved shelf life over other finishes. These finishes are also free of ionic contaminants, compatible with most flux chemistries, and smoother than HASL. Nickel-gold (Ni-Au) is becoming a common metallization in ball grid array packages with copper solder pads. The outer-most gold (Au) layer protects the pad from corrosion and the nickel (Ni) layer provides the diffusion barrier to inhibit growth of Cu-Sn intermetallics. It is found that, during reflow, the Au layer reacts very quickly with the solder and forms a distribution of $AuSn_4$ precipitates throughout the bulk. As the aging time is increased, the $AuSn_4$ grains begin to separate themselves from the Ni layer at the root of the grains. Finally, when all the Au intermetallic leaves the interface, a Ni_3Sn_4 intermetallic compound starts forming at the interface. The growth rate of Ni_3Sn_4 is initially linear and decreases with time. However, research work done by Mei et al.[33] revealed a peculiar phenomenon in the case of Ni-Au metallization. It was found that after extensive aging, at 150℃ for 2 we eks, the Au-Sn intermetallic redeposited onto the solder substrate interface. This layer was weak and the solder joint failed by a brittle fracture along the surface between the redeposited layer and the Ni_3Sn_4 layer that was formed during reflow. The effect of gold thickness on the solder joint is well documented. The limit of 2.5-3% weight of gold is usually expected to be the upper limit to cause joint failure [33]. A study by

Huang et al. [34] revealed that thicker gold plating showed higher ball shear force; this was related to a phenomenon called "precipitation hardness". But after reliability tests, the effect of this phenomenon vanishes and the Au-Sn or Sn-Ni intermetallic compounds dominate ball shear force. Thus, thicker gold plating should reduce the shear force of the joint. They observed the failure to occur in the solder when the gold plating is thin and along the interface of Au-Sn intermetallic when the gold plating was relatively thick.

<u>2.3 SAC Solder Microstructure Evolution</u>

2.3.1 Lead Free Solder Microstructure

There have many studies that investigate the variation in solder microstructure. One of the examples studied the BGA packages assembled on a PCB using a reflow process with a cooling rate from melting temperature typically under 4°C/s. The presence of additional components on the PCB lowers the cooling rate even further to less than 2°C/s. A typical solder joint exposed to such low cooling rates have very few grains [10]. Each Sn grain is found to be made up of colonies of β-Sn dendrites and Sn-Ag-Cu eutectic. The Sn-Ag-Cu eutectic regions consists of Sn, Ag_3Sn and Cu_6Sn_5 precipitates. These precipitates are in needle form and appear as particles in a cross-sectional image. Similar studies found that undercooling plays an important role in the final microstructure of the solder alloy. Undercooling is a phenomenon where a substance retains its liquid state well below its freezing temperature. Sn is known to exhibit significant undercooling amounting to over 25°C [35, 36]. The Ag_3Sn and Cu_6Sn_5 precipitates on the other hand have very low undercooling amounting to only few degrees [36]. When cooled at a slow rate, some of these precipitates have sufficient time to grow in the form of plates [37], as shown in Figure 2.9, before Sn dendrites starts to nucleate. The locations at which the Ag_3Sn plates are formed are random and cannot be predicted.
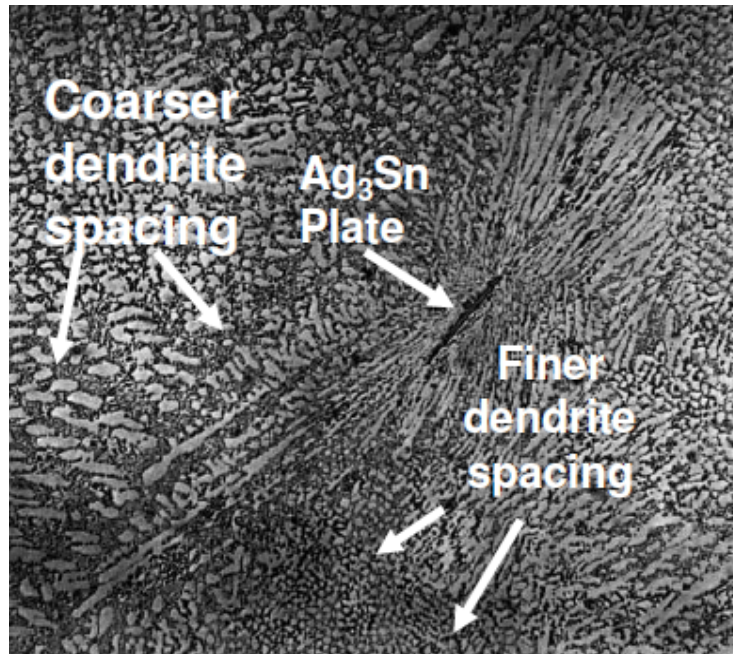
Figure 2.9. Dendrite spacing in a SAC solder joint [37]

2.3.2. Quantifying the Lead Free Solder Microstructure

There are different ways to characterize and quantify the microstructure of SAC alloy. These microstructural parameters can be monitored at regular intervals during aging or field-use conditions and the reliability of the solder joint can be determined. The following are the possible parameters that can be used for monitoring microstructural evolution:

- Grain size

- Dendrite arm spacing

- Intermetallic growth at the solder joint and copper pad interface

- Ag_3Sn and Cu_6Sn_5 Particle coarsening

Grain boundaries store energy and when a solder alloy is subjected to thermomechanical loading, the grain tends to grow to lower the grain boundary surface area and hence the stored energy. The method however cannot be used to monitor the microstructure evolution for the SAC solder alloy because given the slow cooling rate, the solder

joints have very few grains in a cross-section. Any increase in grain size will be too small to be detected.

Dendrite arm spacing is another metric used to quantify the microstructure. The dendrite arm spacing is not constant within a solder joint. It varies widely within a solder joint and around the Ag_3Sn plate region as shown in Figure 2.9. Moreover, Gibson et al [38] have also reported that aging at 120°C for 100 hours makes the solder joint lose its dendrite structure.

The copper pads on which the solder joints are reflowed usually have an organic protective coating to protect the copper pads from oxidation. During the reflow process, the solder alloy dissolves the organic protective coating and wets the copper pad. A Cu_6Sn_5 intermetallic compound (IMC) layer is then formed at the interface. This layer is known to grow significantly with thermal treatment and has been used as a parameter to monitor microstructure evolution [39]. Increased IMC growth increases the chances of brittle failures. Therefore, the organic protective coating is now being replaced with Ni/Au under bump metallurgy (UBM). The Au acts as a protective coating preventing oxidation of the copper pad and Ni acts as a barrier preventing migration of copper from copper pads into the molten solder. This reduces the IMC thickness considerably. The IMC has $(Cu_xNi_{1-x})_6Sn_5$ composition [40] with Cu obtained not from copper pad but from migration from the solder alloy to the solder-Ni/Au interface. Subjecting the package to thermal treatment leads to growth of the intermetallic compound. This growth rate is however considerably lesser than the growth rate observed when no Ni/Au UBM is used. Arulvanan et al [41] has shown that the $(Cu_xNi_{1-x})_6Sn_5$ IMC in a BGA package grows less than 10% when subjected to 3000 accelerated thermal cycles between -40°C to 125°C. For more benign field-use conditions, the IMC growth rate will be much slower than during the accelerated thermal cycling.

These reasons make using the IMC growth rate as a parameter to monitor microstructure evolution for field-use conditions not a good choice.

CHAPTER 3

EXPERIMENTAL PROCEDURE

3.1 Sample Preparation

The PBGA package used in this research is the package that is assembled at Cisco System Co. The images of PBGA package and material specifications used in this assembly are represented in the figure 3.1 and the table 3.1. As briefly introduced, solder joint consists of Cu pad, EMIG (Electroless Ni/ Immersion Gold) and Pb-free solder ball. Solder ball is a lead free solder based on Sn-3.0Ag-0.5Cu (SAC305) ternary alloy. There are two interfaces in this assembly, one at the board side and the other at the chip side. The board side is made of Cu pad. Prior to soldering, the Cu pad is treated with Organic Solderabilty Preservative (OSP) to preserve serine Cu surface. On the chip side, Cu trace is treated with Electroless Nikel/ Immersion Gold (ENIG) surface finish, resulting multi-layers consisting of Cu/Ni/Au. Such layers along with solder are shown in figure 3.2 and figure 3.3.

Dwell time and cooling speed applied to each chip in soldering might not be always consistent during assembly process. In particular, there may be a significant cooling rate dependence on the location of solder within a chip. To minimize the influence from such variations, specimens are collected from each chip with a division up into 25 pieces. Then, only the solder joints that are located at the outmost area of the chip are collected for microstructure study because they are likely to have similar as-cooled microstructure with similar cooling rate. These pieces have 5 ~ 6 individual solder joints, as shown in the figure 3.1. Aging treatment is conducted in a convention oven with the target temperatures of 100°C and 150°C for duration of 100, 200, 350, 500, and 1000 hours. "Blue M" oven manufactured by LR Environmental Equipment company is used for the aging treatment.
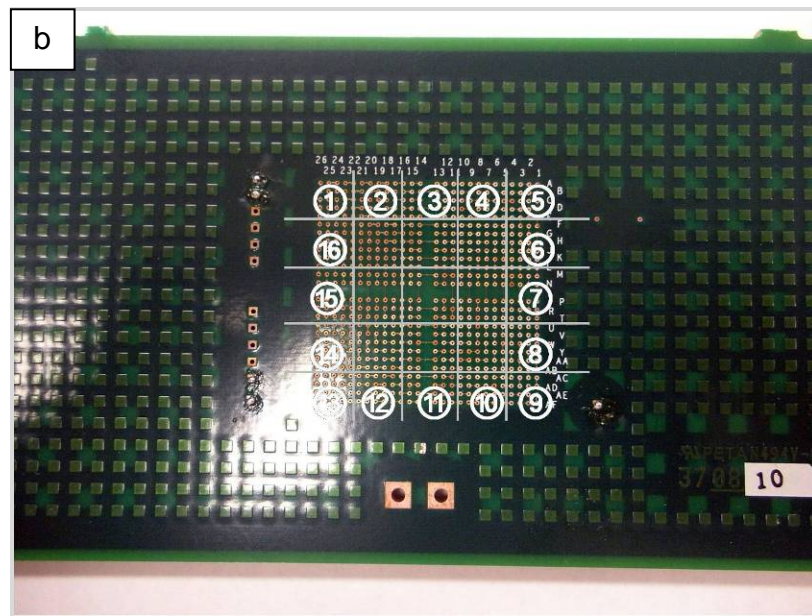
Figure 3.1 Pictures showing (a) PCB board (b) Configuration of specimens

Table 3.1 PBGA Package Standard

Body Size	Ball Count	Ball Pitch	Ball Matrix	Ball Diameter	Mold Cap Thickness	Total Package Thickness
27.0 × 27.0 (mm)	676	1.00 (mm)	26 × 26 F	0.63 (mm)	1.17 (mm)	2.09 (mm)
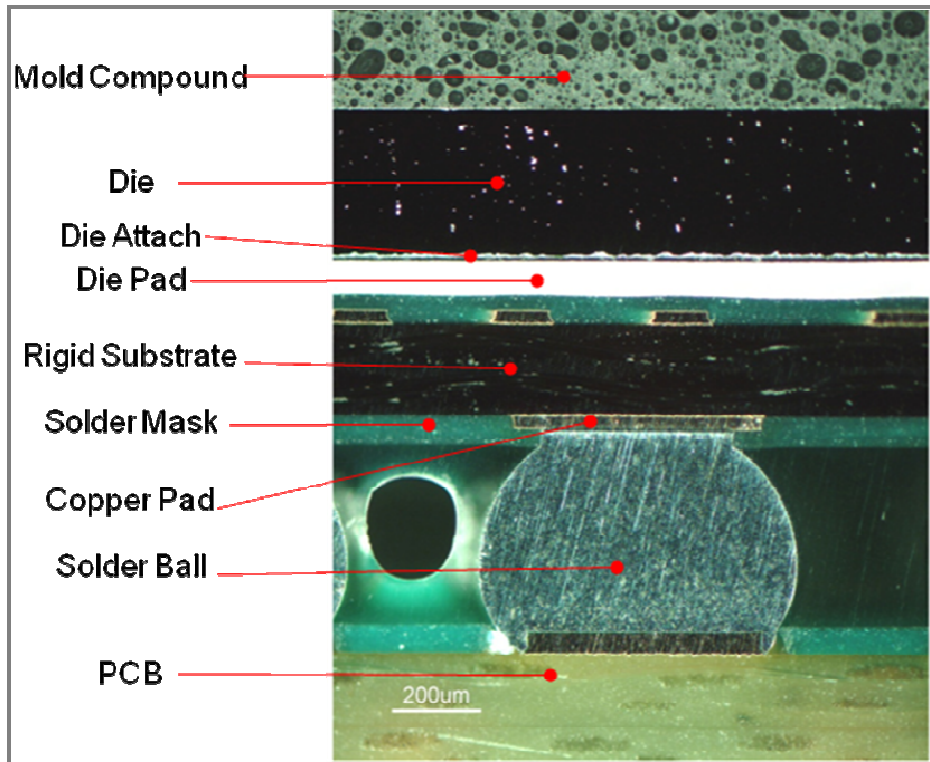
Figure 3.2 Cross Section of PCB board
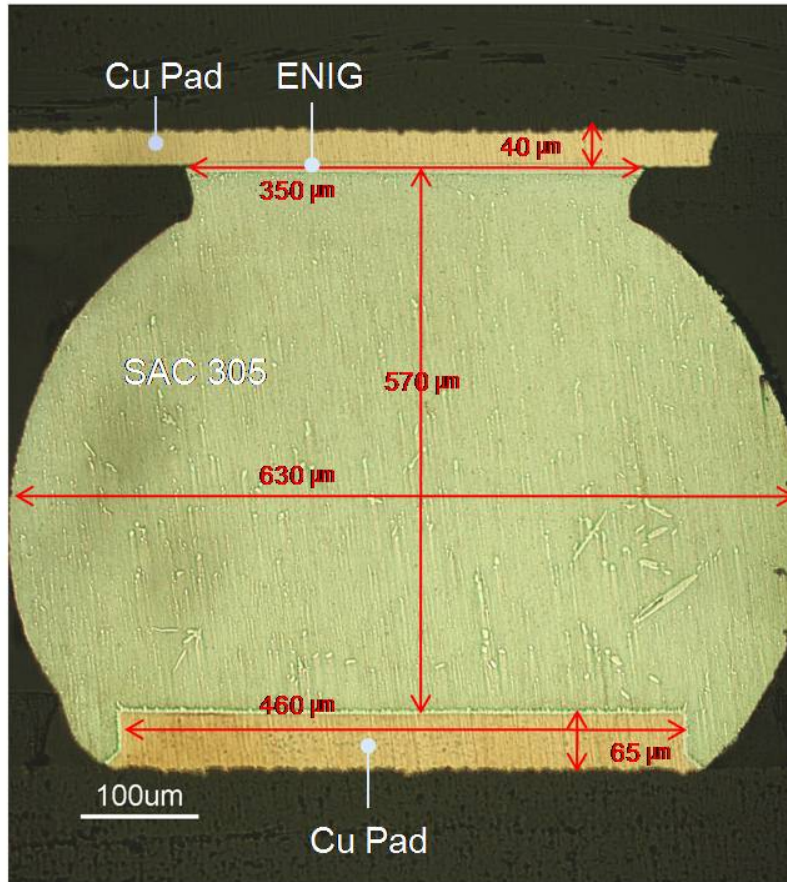
Figure 3.3 Cross Section of Solder Joint

3.2 Microstructure Observation

To observe the microstructure, specimens were prepared by placing solder joint in a resin mount. The specimen was then polished with sand paper 200, 400, 1000, and 1500 grit, followed by micro-polish with alumina powders in size of 20, 5, 1, and 0.3 μm. To reveal microstructural features, the polished sample surface was etched for 5 to 10 seconds using etchant HCl: C_2H_5OH = 2:98. The interface and solder matrix was observed using OM (Nikon Eclipse ME600) and SEM (Hitachi S-3000N Variable Pressure SEM).

In the microstructural characterization, special attention was paid to the following two areas:

1) Growth of $(Cu_xNi_{1-x})_6Sn_5$ IMC in Ni layer/ solder interface, and Cu_6Sn_5 in Cu pad/ solder interface;

2) evolution of Sn-dendrite and the eutectic microstructure;

3.3 X-ray Mapping and Measurement of Phase Volume Fraction

X-ray mapping of Sn, Cu, Ag, Ni elements was performed to observe variation of Cu_6Sn_5 and Ag_3Sn in Interfacial IMC and solder matrix, and to observe movement of alloy elements in each phase. This mapping was performed in at varying magnifications, 3000, 1500, and 500 to enhance the accuracy of phase measurement. After each constitutional phase was identified, volume fraction of phase is measured with an image analyzer (image pro plus).

Variation of elements in IMC was also tracked by conducting interfacial IMC mapping. X-ray mapping was also used to track the variation of the elements in dendrite and eutectic pool consisting solder matrix and precipitation. Particular attention was paid to the characterization of Cu_6Sn_5 volume fraction and its variation in solder matrix.

CHAPTER 4

RESULTS

4.1 Introduction

Current chapter presents the results of the experimental observations with a specific emphasis on the microstructural evolution of SAC305 solder joint with aging treatment at 100°C and 150°C. Since these temperature are considerably high compared to the melting temperature of the given alloy, 220°C, significant microstructural change was anticipated by aging [42]. The microstructural change with aging was indeed noticeably significant.

The microstructural changes in solder joint with aging can be summarized in three main categories. The first is the changes of morphology and thickness of the interfacial IMC. The second is the morphological changes of the dendrite and eutectic pool. The third is the precipitation and the following growth of Cu_6Sn_5 in the solder matrix. These changes are presented in this chapter starting from the results seen in solder matrix to Cu and Ni/solder interface.

4.2 Solder Matrix Microstructure Evolution

4.2.1 As-reflowed Microstructure

In order to closely track the microstructural evolution with aging, the microstructure of as-reflowed solder joint was investigated in detail. This, characterization of the as-reflowed microstructure, enabled not only the metallurgical understanding of the solidification process of the solder but also its influence on the direction of microstructural evolution with aging.

As shown in Figure 4.1, the microstructure of solder joint can be divided into the three main parts: (1) solder matrix, (2) Ni layer/solder interface, and (3) Cu pad/solder interface. The first focus of the investigation was the microstructural characteristics of solder matrix. The

optical micrographs on the Figure 4.1 show that solder matrix consist of β-Sn, eutectic pool and inner IMC. Among these, primary dendrite (β-Sn) occupied the most solder matrix while eutectic pool, visible at the boundaries of β-Sn dendrites, occupied the rest. It was also noticed that well-facetted Cu_6Sn_5 formed and existed within β-Sn dendrite.

According to existing studies, the solidification microstructure of SAC 305 bulk alloy is composed of the primary dendrite β-Sn, Ag_3Sn and the ternary eutectic consisting of Ag_3Sn, Cu_6Sn_5, and Sn phase. The microstructure of solder joint investigated in this study appears to show the similar microstructure. In order to verify it is the same microstructure, x-ray mapping was conducted at magnification 1500X and 3000X. As shown in Figure 4.2, β-Sn dendrite can be easily distinguished from the eutectic pool. However, microstructural features that are different from the previous studies were found when closer inspection of the eutectic pool was conducted. In eutectic pool, while Ag_3Sn and Sn was clearly discerned, Cu signal intensity was found to be very weak. Such result is shown in figure 4.3. The X-ray mapping conducted at 7000X; showed that the weak Cu intensity originates from the Cu_6Sn_5-like particles that are located mainly along the boundary of the eutectic pool. Unlike the previous report where Cu_6Sn_5 phase in Sn-Ag-Cu eutectic is well developed with characteristic facets, these particles were found to have irregular size and shape. One the other hand, Ag_3Sn phase was clearly visible and regular spaced with Sn phase. This microstructure appears to suggest that the eutectic phase seen in the current study may not be fully developed ternary eutectic where well developed Cu_6Sn_5, Ag_3Sn, and Sn phase should coexist. Rather, the result suggests that the eutectic phase is Sn-Ag_3Sn binary surrounded by Cu-rich interface. As will be discussed in later sections, it is believed that non-equilibrium cooling of solder alloy led to the development of binary eutectic phase. This belief is also substantiated by the aging study where the Cu-rich phase at the eutectic boundary disappears rather than coarsened along with other phases in the eutectic, which is not possible if the Cu-rich phase is part of the ternary eutectic.
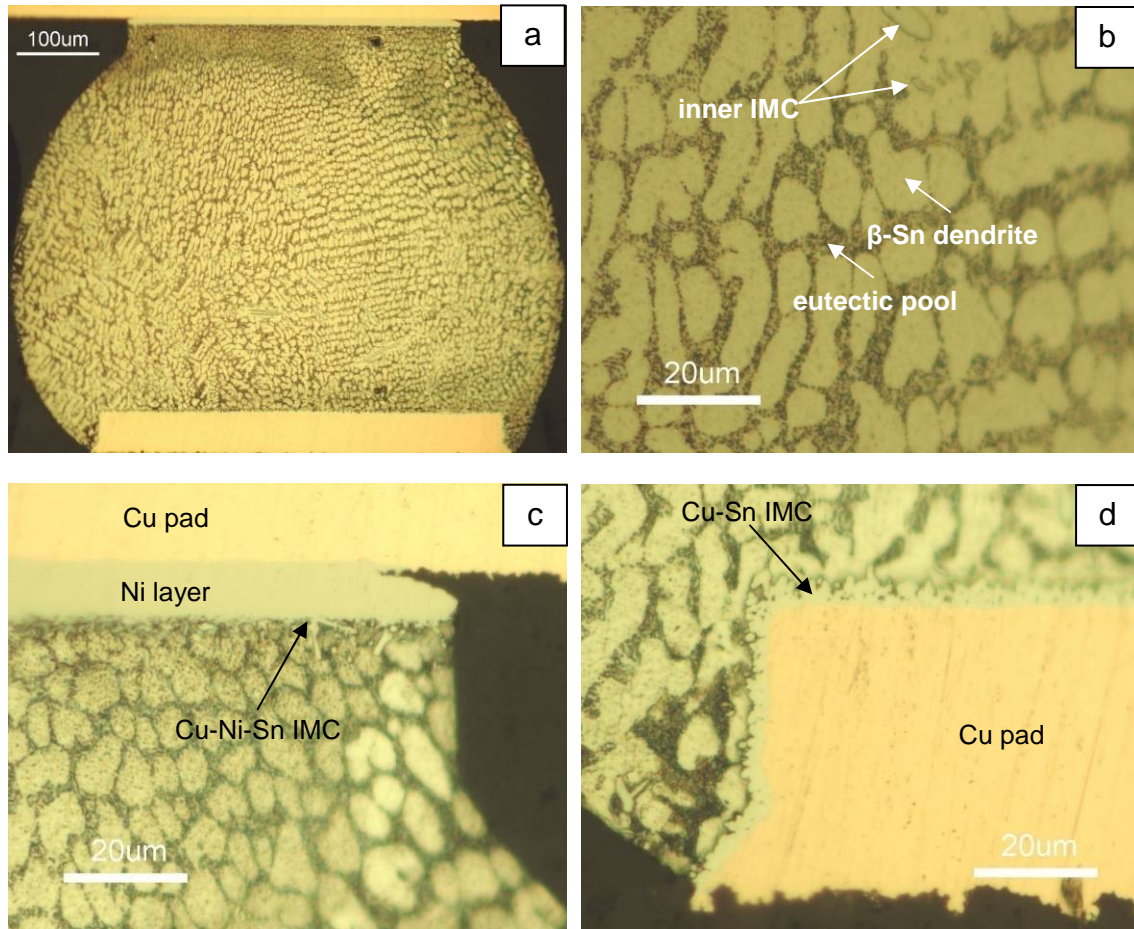
Figure 4.1 optical micrograph showing the as-reflowed structure of a) entire solder joint, b) matrix center region, c) Ni/solder interface, d) Cu/solder interface
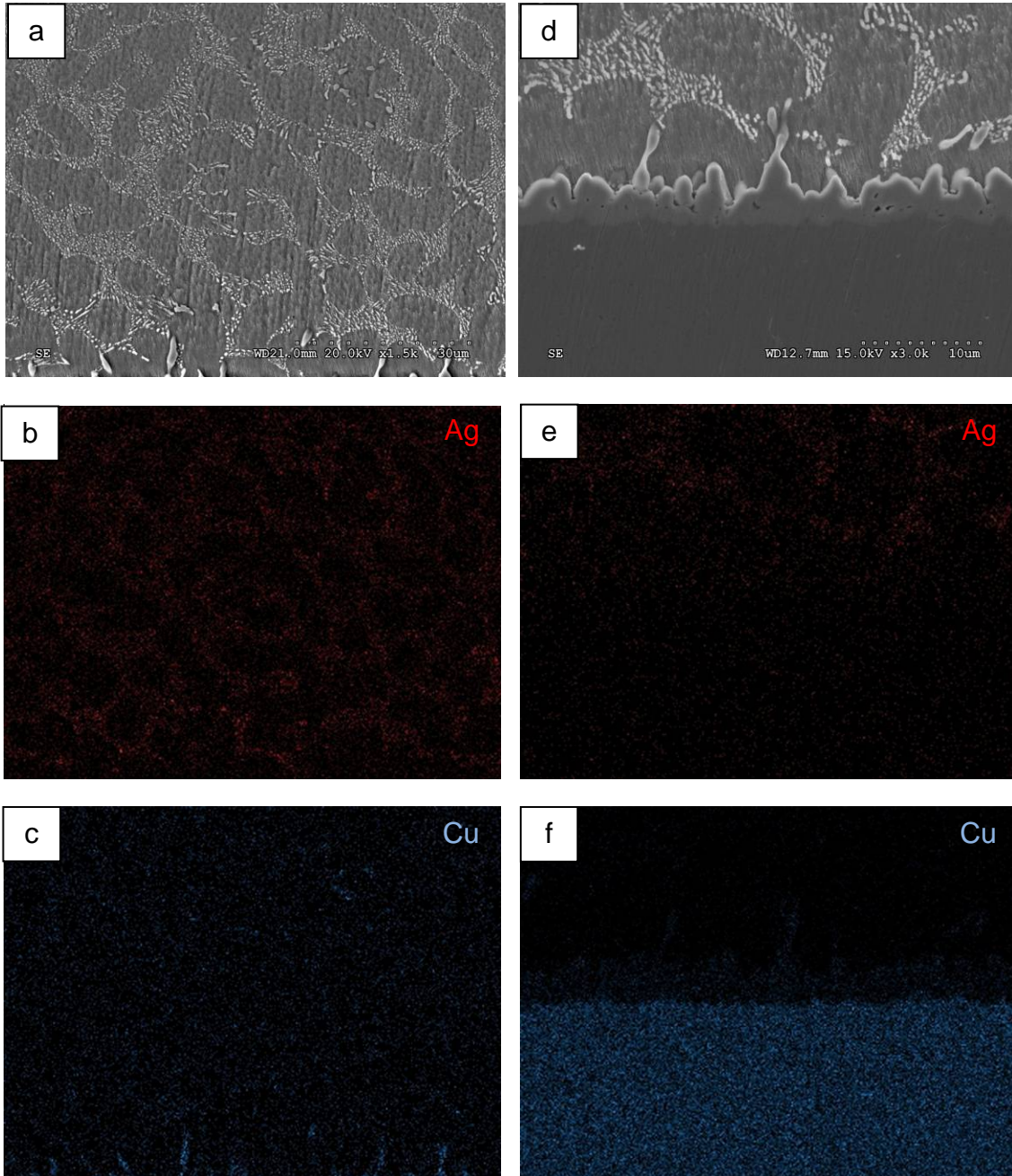
Figure 4.2 X-ray Mapping results and SE image showing absence of Cu-Sn particle in matrix,
a) SE image (×1.5k), b) Ag signal (×1.5k), c) Cu signal (×1.5k),
d) SE image (×3.0k), e) Ag signal (×3.0k), f) Cu signal (×3.0k).
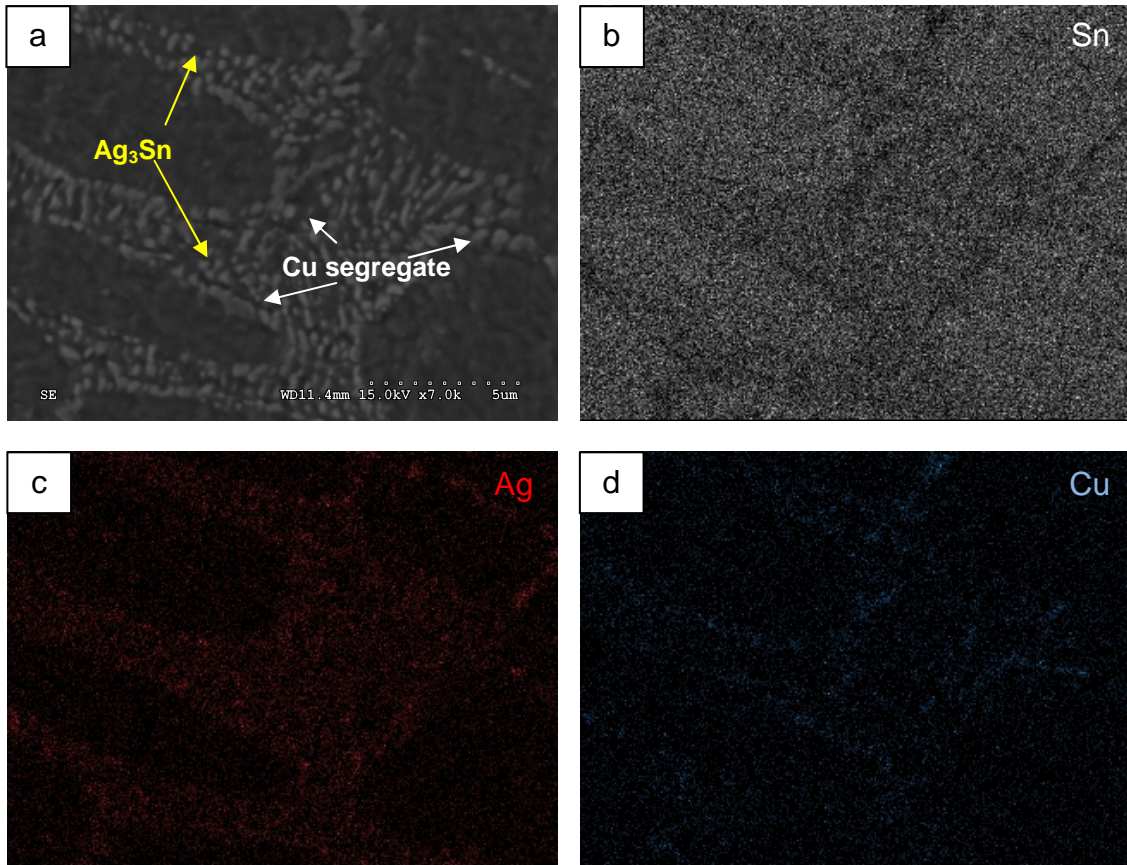
Figure 4.3 X-ray Mapping results (×7000) and SE image showing
a) SE image, b) Ag signal, c) Cu signal,

4.2.2 β-Sn Dendrite Structure and Its Evolution with Aging

As indicated earlier, as-reflowed solder matrix consists of β-Sn dendrite, eutectic pool and inner Cu_6Sn5 IMC. This initial microstructure was found to gradually evolve with aging with a few notable directions. One of characteristics of the microstructural change is gradual collapse of phase boundaries, i.e. boundaries between β-Sn and eutectic as well as between β-Sn dendrites. SE image and X-ray mapping images shown in figures 4.5 and 4.6 represent the collapse of phase boundaries occurring in the solder matrix. From the figures, it can be seen that the boundary between dendrite and the eutectic is clearly visible at as-reflowed condition. However, as aging progresses, the boundaries are becoming faint. The disappearance of the phase boundaries became more evident with longer aging time and at higher aging temperature. The collapse of the dendrite structure resulted by disappearance of phase boundaries was clearly evident when the solder was aged at 150°C f or 200hours or more.

Along with the collapse of β-Sn dendrite, the Cu-rich phase decorating the eutectic boundary was found to disappear. On the contrary, the other two constituents of the eutectic pool, Ag_3Sn and Sn, remained intact and showed only coarsening behavior. These results, collapse of the phase boundaries and disappearance of Cu-rich phase strongly indicate that the as-reflowed SAC 305 microstructure investigated here is highly inhomogeneous probably resulted by non-equilibrium cooling.
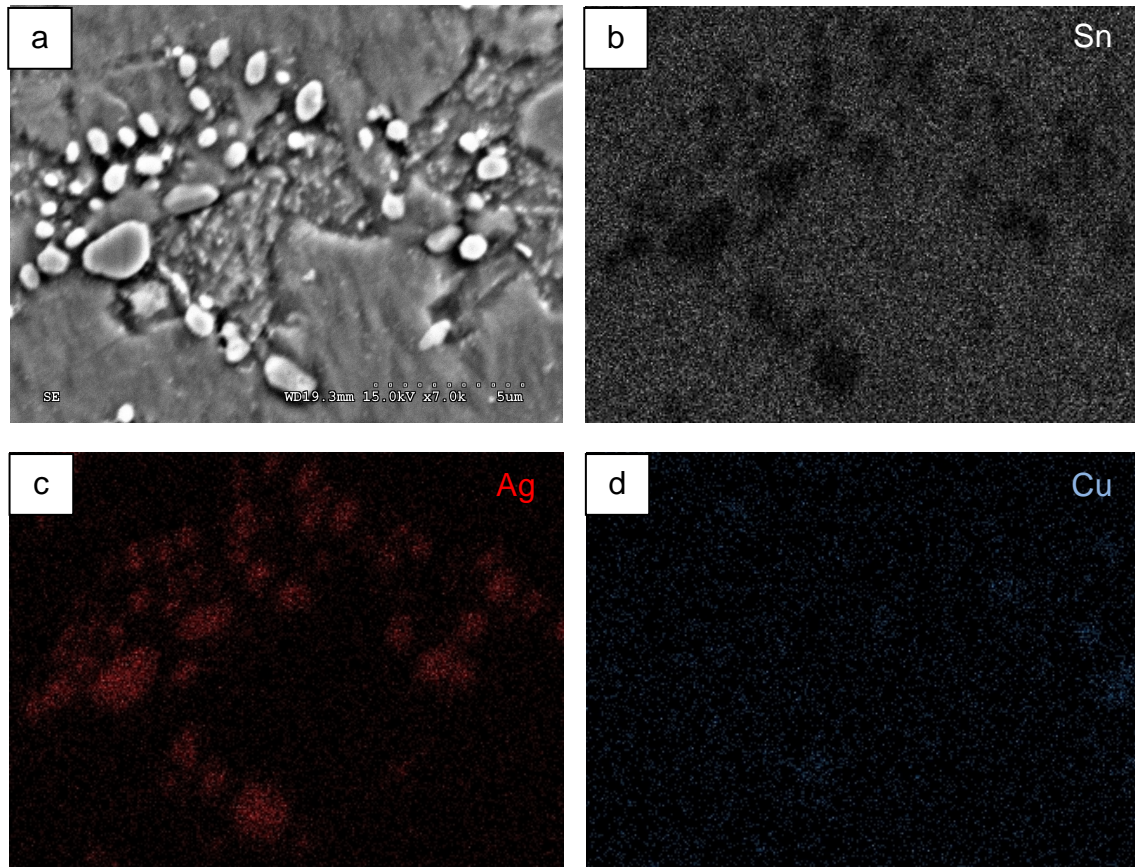
Figure 4.4 X-ray Mapping results (×7000) and SE image showing the area which were eutectic pool a) SE image, b) Sn signal, c) Ag signal, d) Cu signal,
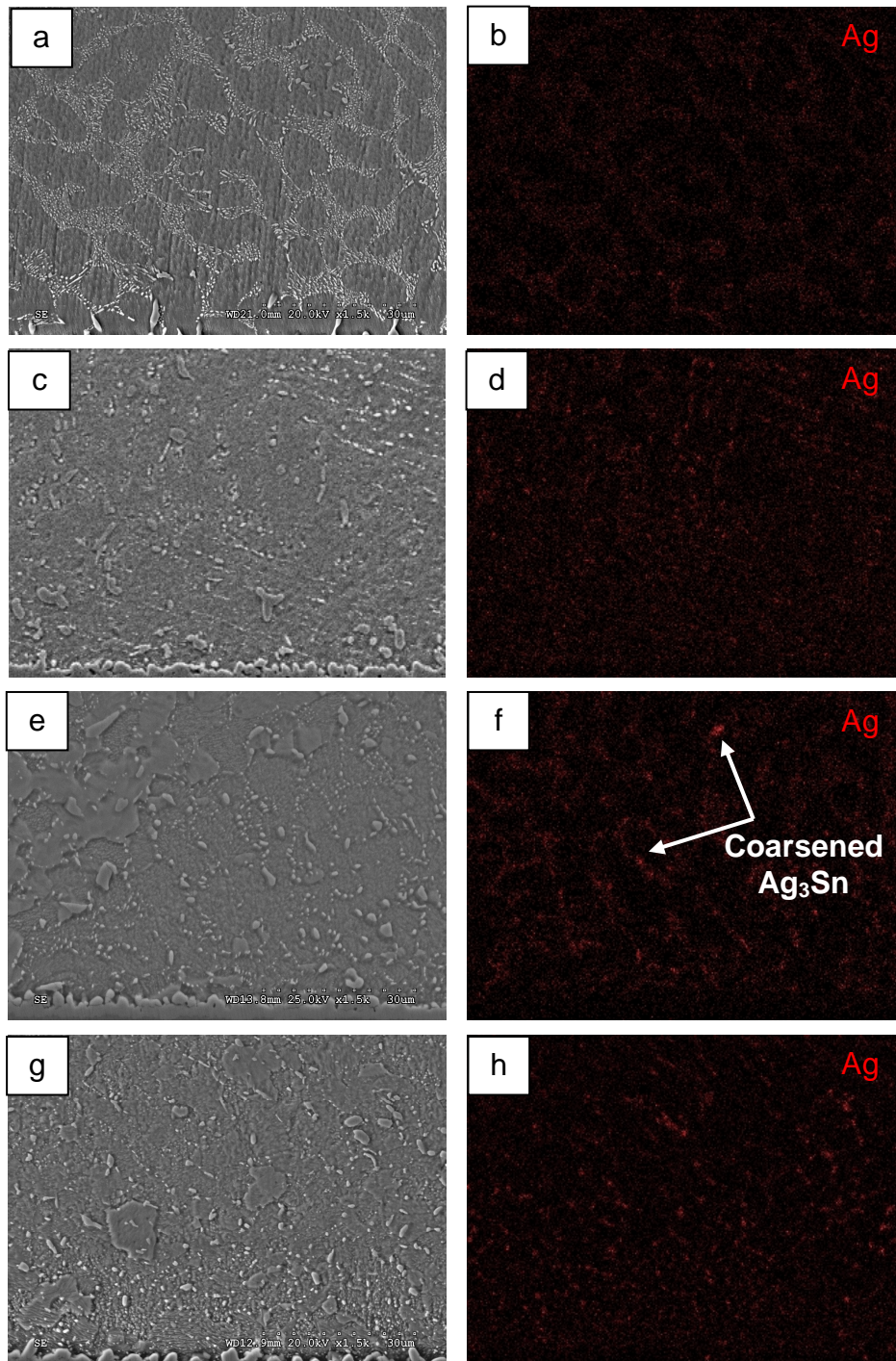
Figure 4.5 SE and Ag x-ray mapping image(×1500) showing dendrite structure change and Ag$_3$Sn coarsening on 100□ aging condition with time followed by; a-b)- as-reflowed, c-d) 100hr, e-f) 200hr, g-h) 500hr
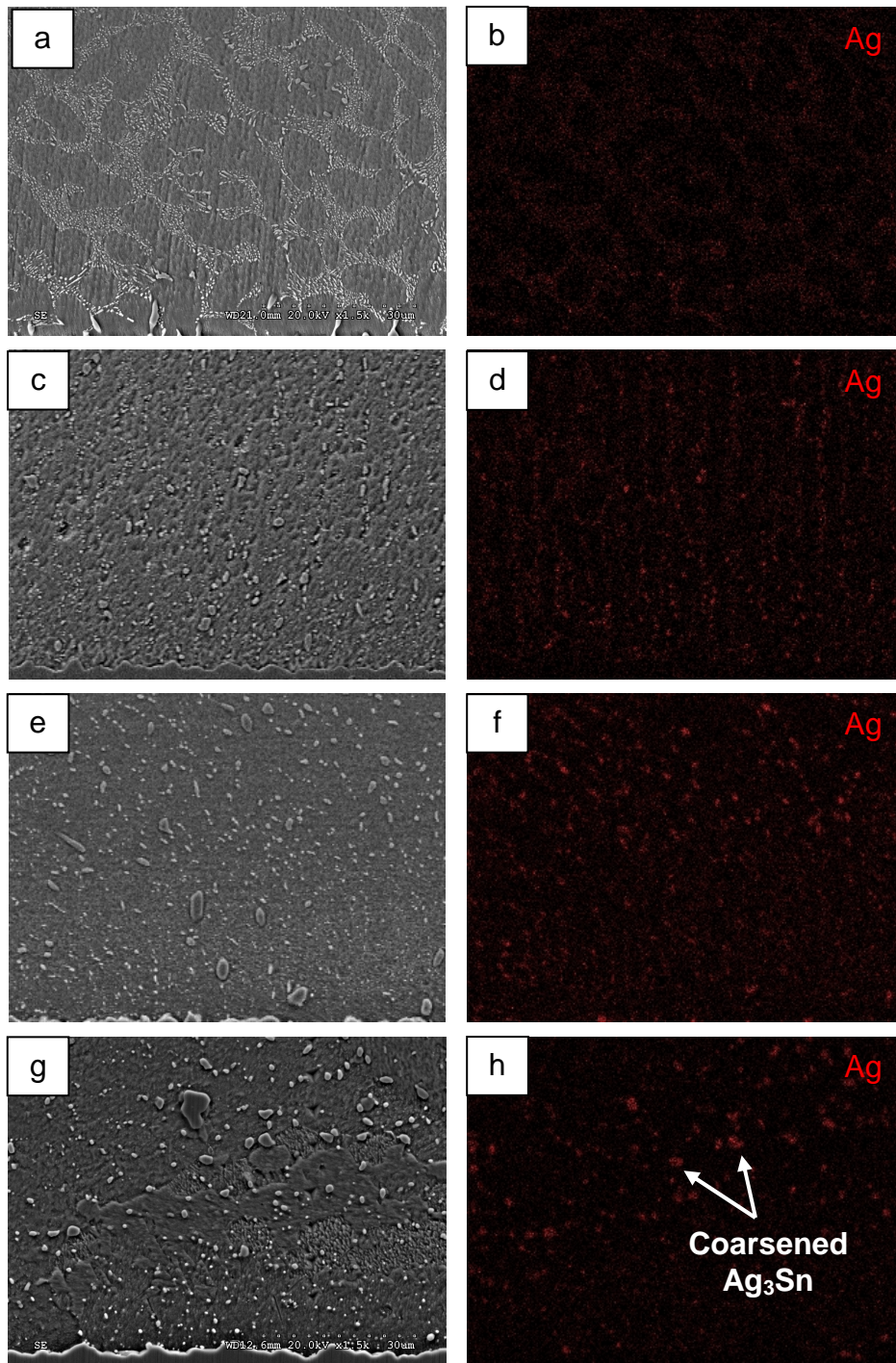
Figure 4.6 SE and Ag x-ray mapping image(×1500) showing dendrite structure change and Ag₃Sn coarsening on 150☐ aging condition with time followed by; a-b) as-reflowed, c-d) 100hr, e-f) 200hr, g-h) 500hr

4.3 Precipitation and Growth Behavior of Cu_6Sn_5 in Matrix

Previous studies have revealed a keen dependence of mechanical properties of near-eutectic Sn-Ag-Cu solder upon its microstructures, such as precipitate size ad number, Sn grain number and orientation, and on the nature of the intermetallic compounds (IMCs) at a solder/substrates interface. The Cu_6Sn_5 and Ag_3Sn precipitates which form in near eutectic Sn-Ag-Cu strengthen the Sn matrix material through a precipitate hardening mechanism: because the they behave as a barrier to motion of dislocations. A large number of uniformly distributed, small precipitates are most effective. For this reason, it is important to understand how IMC phases are distributed in a solder matrix and evolve with aging.

In the present study, it is found that the only phase that was existing in the as-reflowed structure and also evolving with aging is the Cu_6Sn_5 IMC. No Ag_3Sn IMC was found in β-Sn dendrites although they existed in eutectic pool. Further, it was found that the Cu_6Sn_5 phase growth was differently proceeding depending on the location in the solder. At a place close to Cu interface, it was found that Cu_6Sn_5 phase continuously grew with increasing volume fraction. On the other hand, they were also found to grow but their volume fraction was not found to be changed much.

4.3.1 Cu_6Sn_5 IMC in As-reflowed Structure.

On the solder matrix of the as-reflowed sample, the large Cu_6Sn_5 phases were observed inside the β-Sn dendrites, while Ag_3Sn IMCs were hardly seen. Majority of Ag was found in eutectic phase. Figure 4.7 shows the Cu_6Sn_5 IMCs found in β-Sn dendrite. It can be seen that they are well grown and well-faceted. This indicates that the IMC was formed during cooling process. Furthermore, it appears that it is the phase that solidifies the first. This belief is based on the fact that the Cu_6Sn_5 IMC is not located in-between the dendrite but within the dendrite. Microstructure suggests that the Sn dendrite starts from IMC. This indicates that Cu_6Sn_5 solidified first and β-Sn dendrite formed later. Hence, the solidification sequence of the alloy appears to be

$$L \rightarrow L + Cu_6Sn_5 \hspace{4cm} (1)$$

$$L + Cu_6Sn_5 \rightarrow L + Cu_6Sn_5 + \beta\text{-Sn} \hspace{2.5cm} (2)$$

$$L + Cu_6Sn_5 + \beta\text{-Sn} \rightarrow Cu_6Sn_5 + \beta\text{-Sn} + \text{binary eutectic } (\beta\text{-Sn} + Ag_3Sn) \hspace{1cm} (3)$$

This solidification sequence is different from what is found in the previous studies on the bulk alloys. In those studies, it is suggested that the primary solidification phase is β-Sn, followed by Ag_3Sn and eutectic, that is

$$L \rightarrow L + \beta\text{-Sn} \hspace{4cm} (4)$$

$$L + \beta\text{-Sn} \rightarrow L + \beta\text{-Sn} + Ag_3Sn \hspace{2.5cm} (5)$$

$$L + \beta\text{-Sn} + Ag_3Sn \rightarrow \beta\text{-Sn} + Ag_3Sn + \text{ternary eutectic } (\beta\text{-Sn} + Ag_3Sn + Cu_6Sn_5) \hspace{0.5cm} (6)$$
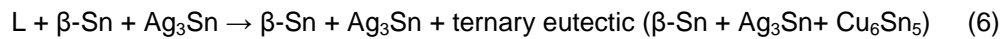
The expected microstructure of SAC305 alloy following solidification sequence (4)-(6) would consist of β-Sn dendrite, Ag_3Sn IMCs located at the dendrite boundary and the ternary eutectic. However, the microstructure investigated in this study is markedly different. It suggests that the alloy composition is changed during reflow process, probably enriched with Cu due to reaction of Cu pad.
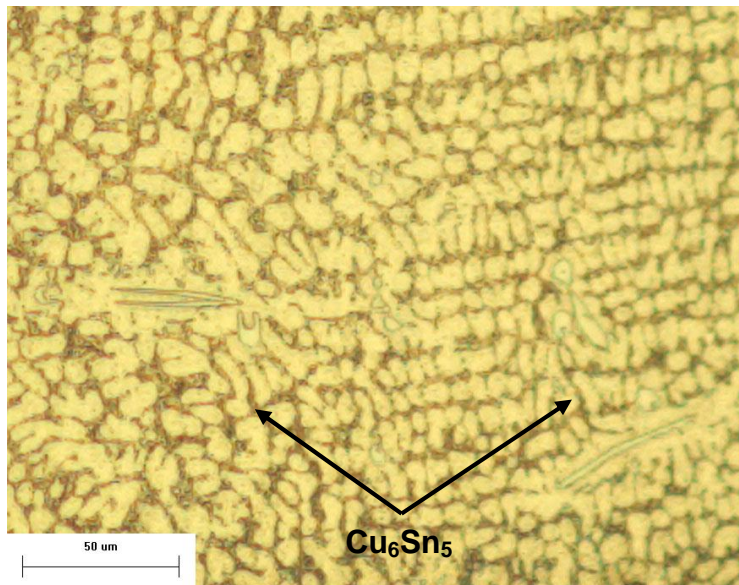

Figure 4.7 Optical micrograph showing the position of Cu_6Sn_5 within dendrites

43

4.3.2 Cu₆Sn₅ Precipitation and Growth in Solder Matrix

On the as-reflowed structure Cu_6Sn_5 particles were found to be mainly distributed in the Sn dendrite. Although the specimens were aged at the elevated temperature and the expanded time, most of Cu_6Sn_5 particles were positioned in the dendrite while only small portion of them was found at inter-dendritic region. This indicates that Cu_6Sn_5 mainly precipitates and grows in the dendrite.

The basic requirement for the precipitation reaction is a lower solubility at lower temperature. Sn-Cu phase diagram for SAC 305 alloy shows that the solubility of Cu in Sn rapidly decreases with decreasing temperature. Therefore if melted solder ball is rapidly cooled to room temperature, it is expected that Cu becomes supersaturated in β-Sn matrix. The supersaturated Cu is then precipitate out in Sn matrix with aging. These small sized Cu_6Sn_5 precipitates are then expected to coarsen as aging progresses. It is indeed the case found in the present study. However, the precipitation and growth behavior was found to be different at two interfacial regions of solder joint, Cu side and Ni side. Furthermore, it is found the main part of growth is actually resulted by supply of Cu from Cu pad.

Figure 4.8 shows Cu mapping result of specimen under aging at 100℃; Figure 4.8 a-d shows Cu mapping results of Ni/solder interfacial region under aging and Figure 4.8 e-h are of Cu/solder interfacial region when aged at 100°C. The bright contrast area corresponds to Cu_6Sn_5 phase. It can be seen that Cu_6Sn_5 phase volume fraction is clearly different at two interfacial regions. The fraction of Cu IMC is clearly higher in Cu side of interface. Note also that its volume fraction increases with aging time. On the other hand, Cu IMC at Ni side of interface tends to grow but its volume fraction is not changed much. The same trend was found in samples aged at 150°C, which is shown in Figure 4.9.

The change in the IMC volume fraction at both sides of interface area quantified and summarized in figure 10. It can be seen that the volume fraction of the Cu_6Sn_5 IMC increases at the solder near Cu pad side increases with aging time. Higher aging temperature makes the

44

growth rate to be faster. On the other hand, the Cu IMC near to Ni pad grows very little at both temperatures. With increase in the volume fraction of IMC near Cu pad side, the total amount of Cu IMC in entire solder is found to increase with aging. This result creates a fundamental question, which is where the extra Cu originates from. One can argue that the increase in the volume fraction could be resulted from precipitation and growth of supersaturated Cu. However, it is believed that such contribution to total increase in volume fraction seen in this study is minor, if any. If it is the precipitation and growth of supersaturated Cu, it is expected that Ni side would exhibit the similar rate of IMC volume fraction increase at both side of solder. However, it is found that Cu pad side is the only area where Cu IMC fraction is increased. Also, the average fraction of Cu IMC was found increase with aging, more at higher aging temperature. This means that an additional Cu was supplied to solder to result in increase in Cu IMC volume fraction. It is our belief that the additional Cu came from Cu pad, as a result of Cu diffusion into solder matrix. Since Ni acts as an effective diffusion barrier against Cu diffusion, Cu entrance to Ni side of solder should be substantially small, leading to no change in the Cu IMC fraction at Ni side of solder. This result further indicates that the Cu side of solder would have higher mechanical strength than the NI side of solder. This is in fact consistent with the fatigue test result that shows the change in the failure location from Cu pad side to Ni pad side with aging.

Figure 4.8 X-ray mapping image (×500) showing the change of Cu_6Sn_5 volume fraction with 100℃ Aging temperature and a-d) as-reflowed, 100hr , 200hr, 500hr on Ni/solder side, e-f) as-reflowed, 100hr, 200hr, 500hr on Cu/solder side.

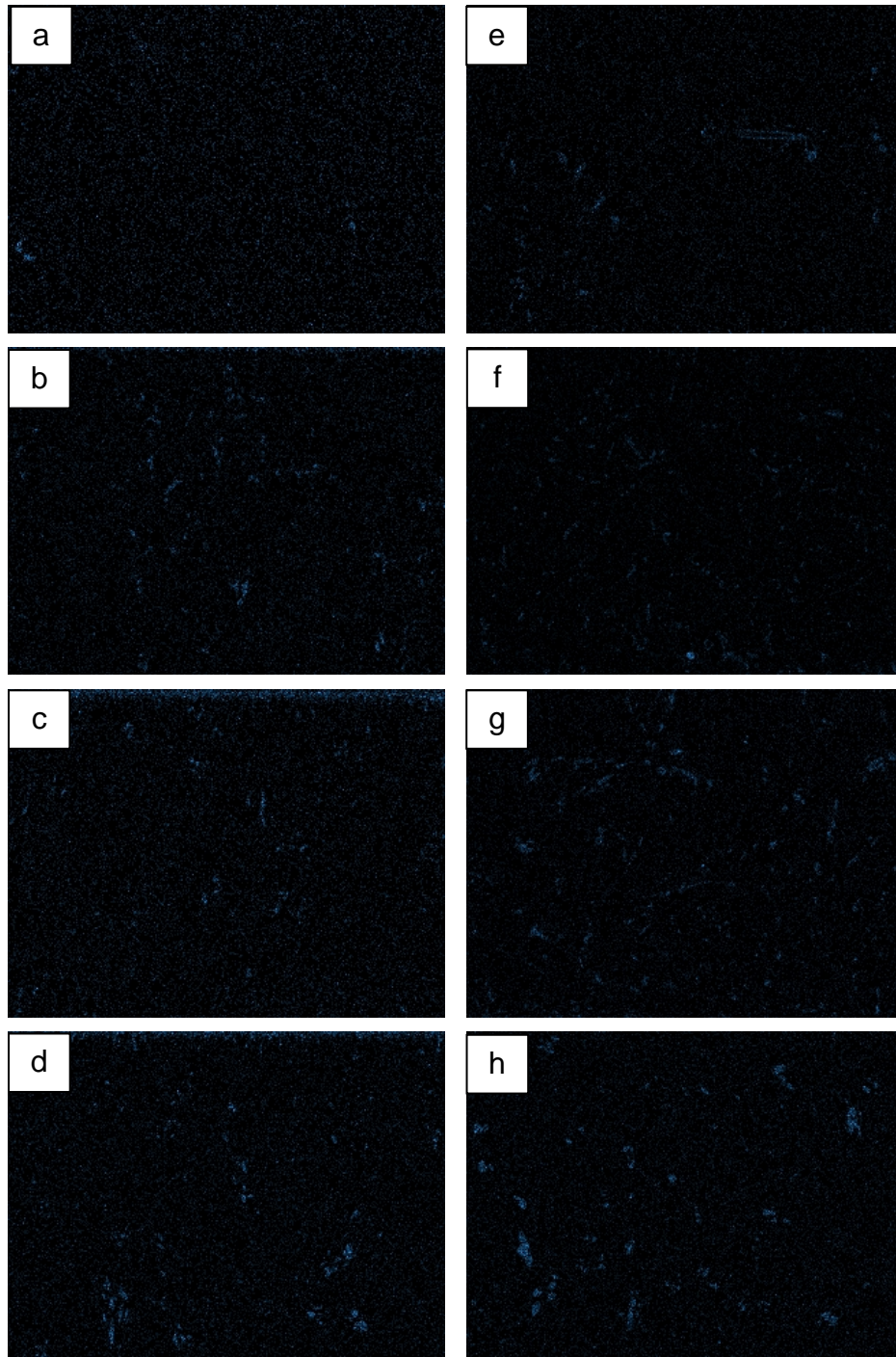Figure 4.9 X-ray mapping image (×500) showing the change of Cu_6Sn_5 volume fraction with 150℃ Aging temperature and a-d) as-reflowed, 100hr , 200hr, 500hr on Ni/solder side, e-f) as-reflowed, 100hr, 200hr, 500hr on Cu/solder side.
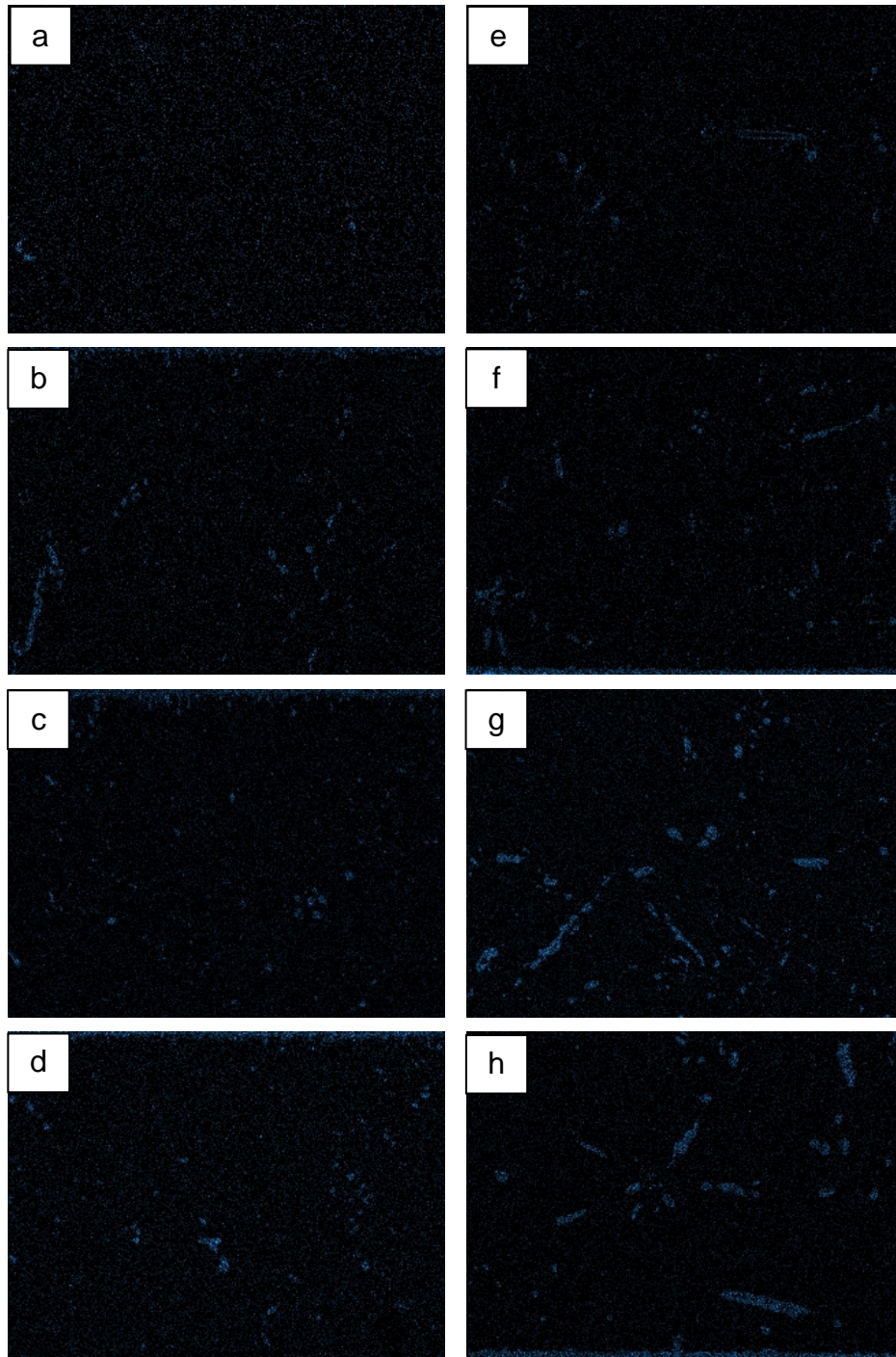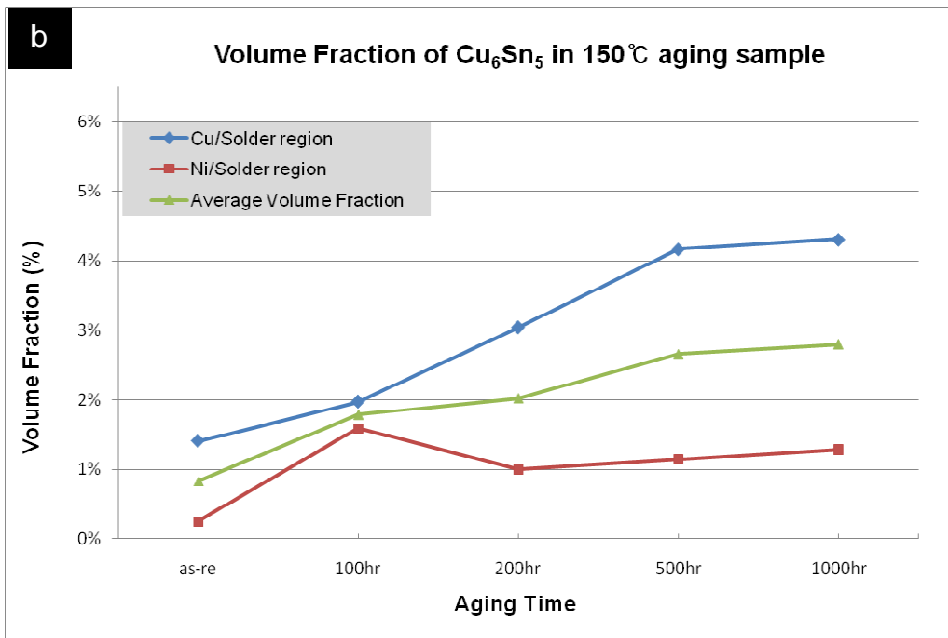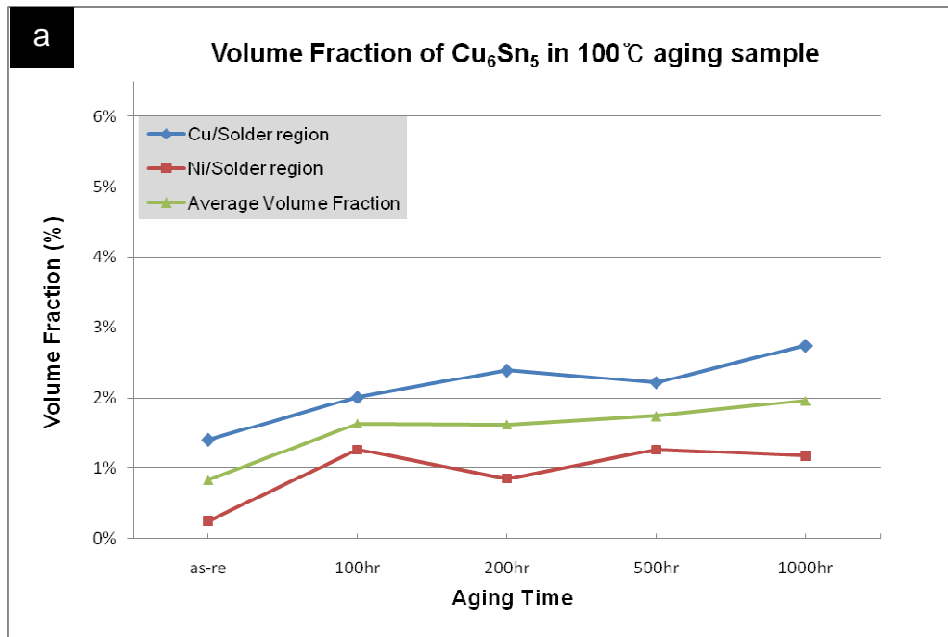
Figure 4.10 quantitative analysis showing the change of Cu_6Sn_5 volume fraction in Ni/solder interfacial region and Cu/solder interfacial region with aging time; a) 100℃, b) 150℃

<u>4.4 Interfacial IMC Growth</u>

As it is shown in Figure 4.1, IMC forms between Cu/solder matrix and Ni/solder matrix interface at as-reflowed state. At Cu/solder matrix interface, a classic scallop-type Cu_6Sn_5 IMC layer forms while in $(Cu_xNi_{1-x})_6Sn_5$ IMC forms at Ni interface. As aging progresses, both IMCs between solder matrix and substrate grow but with different growth kinetics.

4.4.1 Ni/Solder Interfacial IMC Growth

IMC formed at Ni/solder interface, as mentioned in Ch.2, is identified to be $(Cu_xNi_{1-x})_6Sn_5$ IMC. At as-reflowed condition, $(Cu_xNi_{1-x})_6Sn_5$ IMC takes the form of the needle extended toward solder. The aging does not appears to change the size of the needle. Rather, it is found that IMC grows starting from the base of the needle. Therefore, overall thickness of IMC layer, defined as a distance between in Cu/Ni interface and the end of IMC needle, appears to remain constant. Higher aging temperature makes the IMC densification to occur faster. This behavior is shown in figure 4.11.

4.4.2 Cu/Solder Interfacial IMC Growth

Contrast to Ni side IMC, IMC found at Cu side is Ni-free Cu_6Sn_5 IMC having a classical scallop structure at as-reflowed state and is noticeably thicker than $(Cu_xNi_{1-x})_6Sn_5$ IMC at Ni/solder interface. This is consistent with findings made in other studies. Further consistency was found in the aging behavior. Figure 4.12 shows morphology change of Cu_6Sn_5 IMC at aged conditions. It can be seen that as aging proceeds, Cu_6Sn_5 IMC thickens while the surface becomes smoother. Its growth rate is shown in Figure 4.13 in comparison with that of $(Cu_xNi_{1-x})_6Sn_5$ IMC at Ni interface. It can be seen that thickness of Cu_6Sn_5 increases with a rate proportional to $time^{1/2}$, indicating that it is diffusion-controlled process. The rate of growth is higher at higher temperature, which is not surprising considering the fact that diffusion is faster at higher temperature.

Figure 4.11 SE image showing Ni/solder interface change with aging condition of
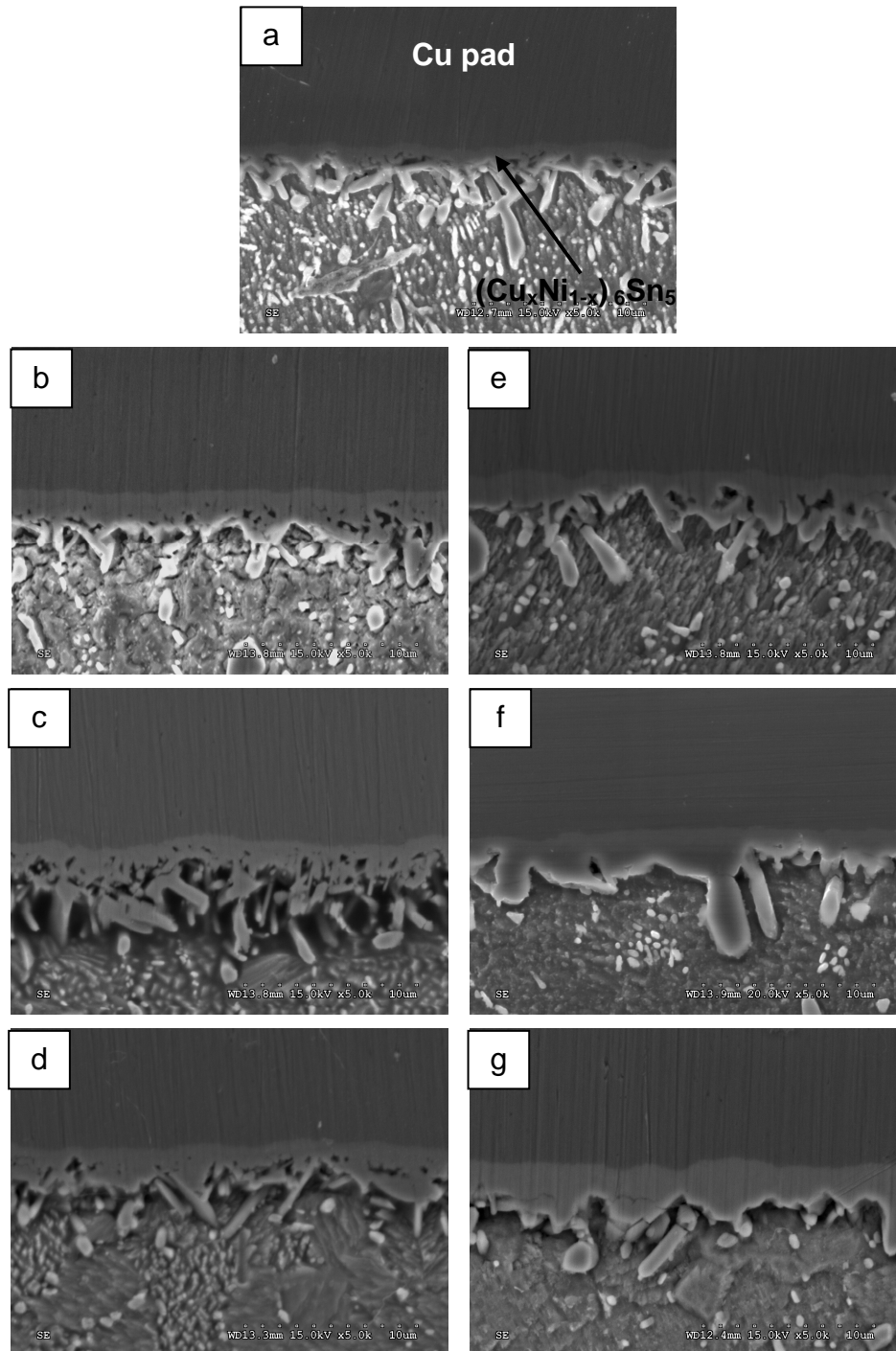a) as-reflowed, b-d) 100hr, 200hr, 500hr at 100℃, e-g) 100hr, 200hr, 500hr at 150℃

50

Figure 4.12 SE image showing Ni/solder interface change with aging condition of
a) as-reflowed, b-d) 100hr, 200hr, 500hr at 100°C, e-g) 100hr, 200hr, 500hr at 150°C
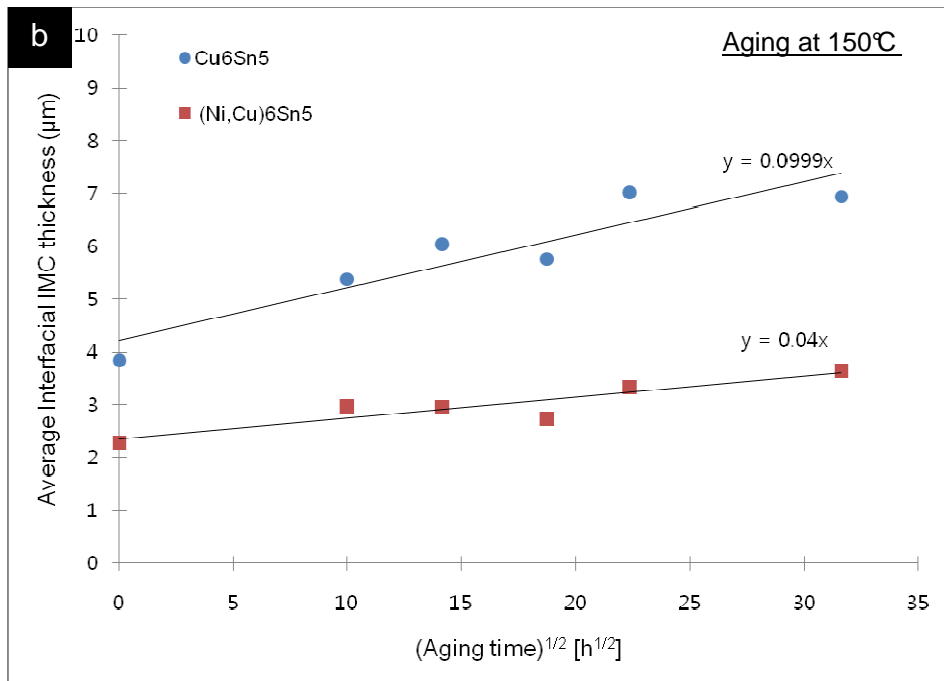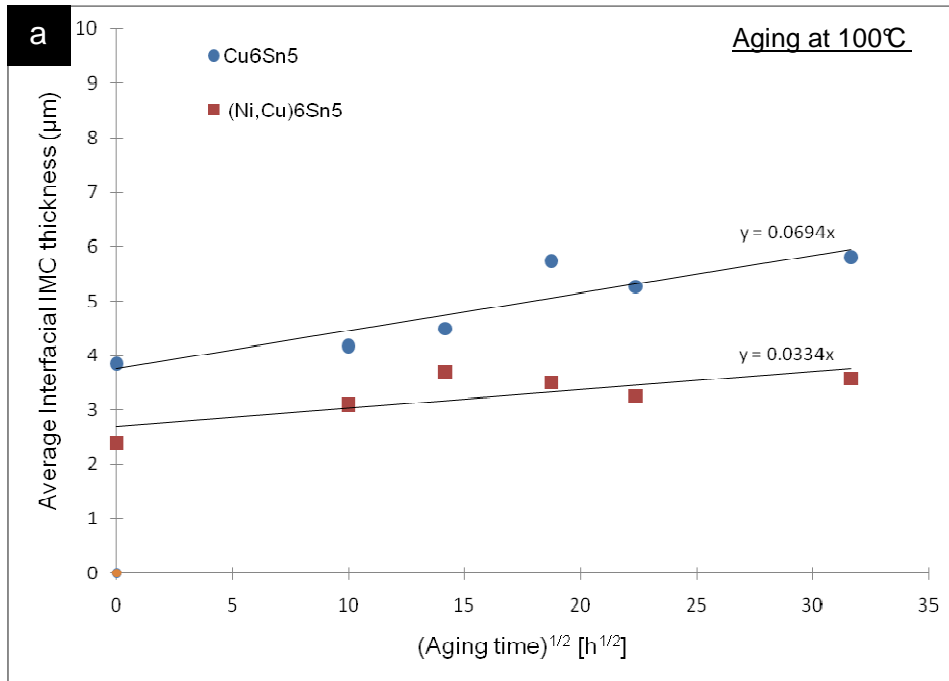
Figure 4.13 Average thickness of IMCs layer at the Ni/solder and Cu/solder interface vs. aging time at a)100℃, b)150℃

CHAPTER 5

DISCUSSION

<u>5.1 Introduction</u>

With an immense importance of solder technology, solder microstructure has been extensively studied in the past. These studies are not limited to the as-reflowed microstructure but include microstructure change with aging treatment. These studies have yielded significant understanding of the metallurgical processes involved in the solder joint, yet this finds that understandings made in prior studies are largely incomplete. Specifically, the present study finds two importance aspects of microstructural characteristics that are different from prior understanding and they deserve further consideration. The first difference is the nature of as-reflowed. Prior studies assume that 1) the joint microstructure is at near equilibrium and 2) solder composition is not affected by reaction with Cu or Ni pad. However, present study finds that those assumptions are grossly wrong. It is found that the reflowed microstructure is at highly non-equilibrium condition, sufficient to alter basics phase make-up of solder microstructure. Instead of ternary eutectic, it is believed that binary eutectic is the normal part of microstructure. Also, it is found that alloy composition is greatly changed by entrance of Cu from Cu pad. This alters the fundamental solidification sequence. With these two, aging response of solder alloy shows very unusual patterns, most notably collapse of Sn dendrite and disappearance of Cu in eutectic boundary and growth of Cu IMC within Sn dendrite. Secondly, it is found that Cu pad is continuously feeding Cu to solder, resulting in enrichment of Cu IMC near Cu interface.

53

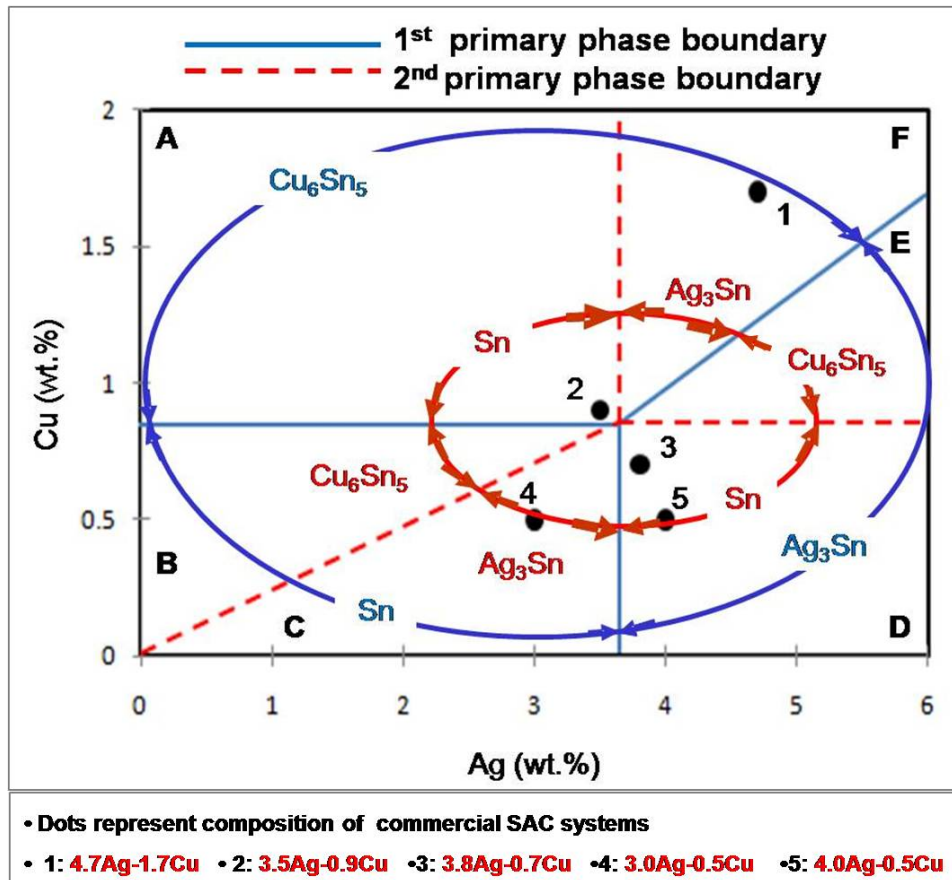<u>5.2 Development of As-reflowed Microstructure</u>

The first characteristic feature of the as-reflowed microstructure is the presence of Cu_6Sn_5 IMC embedded within β-Sn dendrite. According to the solidification sequence of the bulk alloy, this phase should not exist within the dendrite. Rather, Ag_3Sn should be the phase located along the boundary of Sn dendrite. The source of such change can be found from the possibility that liquid solder can be enriched with Cu because of reaction with Cu. According to the solidification sequence map suggested by Prof. Kim's prior study (unpublished), the solidification sequence can change with Cu addition. Figure 5.1 shows the solidification sequence of SAC alloys**.** In this plot, X-axis represents composition of Ag and Y-axis represents Cu. The blue line represents the first phase that solidifies upon cooling and the red line represents the second primary phase. It can be seen that the SAC 305 belongs to "C" section where the first primary phase should be Sn and the second should be Ag_3Sn. Note that when the alloy is enriched with Cu while others kept constant, the solidification field shifts to B and A. In section A, the solidification begins with Cu_6Sn_5 followed by dendrite Sn. This matches well with the microstructure investigated in this study. Therefore, it is reasonable to conclude that the SAC 305 alloy used in the assembly became doped with Cu to a degree to be subjected to completely different solidification sequence expected from the bulk alloy. The fact that the solder ball used in the present study is far smaller than the ones used in other studies may explain the difference in result. With small size of solder ball, much greater level of composition change can be resulted even if the processing condition is similar. .

The second characteristics feature of the reflowed microstructure is the fact that the eutectic phase doesn't seem to be ternary but Ag-Sn binary. It is believed to the result of non-equilibrium solidification. It is well known that liquid Sn can show significant level of super-cooling, near 20°C. The extension of liquid phase field below its equilibrium temperature can result in two things. It promotes formation of Sn dendrite with fraction far greater than what is expected from the phase diagram. This is indeed the case found in the present study. The

54

fraction of Sn-dendrite is much higher than the eutectic phase fraction even if the SAC 305 is at near eutectic composition. The second is loss of Cu in the remaining liquid while Sn dendrite growth progresses. The solubility of Cu in Sn is very high at high temperature, far greater than that of Ag. Therefore, Cu is gradually consumed by Sn dendrite growth, while some of Cu and majority of Ag is rejected to the liquid phase. By the time Sn dendrite growth is completed, Cu content at liquid phase is not enough to form the ternary eutectic. Small amount of Cu can exist at the Sn dendrite boundary as a part of accumulation and subsequent solidification. With lack of Cu in the final liquid, eutectic phase forms by binary reaction of Ag-Sn. This seems to be more consistent with the microstructure found in the present study. Schematic representation of this mechanism is displayed in figure 5.2.

Further evidence that the binary eutectic is the eutectic phase formed in the present case can be found from the fact that aging eliminates the Cu segregation at eutectic pool boundary. Since the phase fraction of Sn is more than the equilibrium and this Sn contains non-uniform distribution of Cu (less the core), the first reaction occurs by the reaction is probably the homogenization of Cu. This may disperse Cu away from the eutectic pool boundary, leaving Sn-Ag binary eutectic to coarsen.

The Sn dendrite, being excess in amount, should also undergo rapid evolution with aging. The first visible evolution is the breakage of the dendrite arms, turning dendrite Sn into more equiaxed grains. The second is the reduction of the Sn phase fraction. Since its evolution is compounded with coarsening, it is difficult to characterize. Further study on this may be necessary to understand how non-equilibrium Sn structure evolves with aging.

• Dots represent composition of commercial SAC systems
• 1: 4.7Ag-1.7Cu • 2: 3.5Ag-0.9Cu •3: 3.8Ag-0.7Cu •4: 3.0Ag-0.5Cu •5: 4.0Ag-0.5Cu

Phase field	1st	2nd	3rd
A	Cu_6Sn_5	Sn	Eutectic
B	Sn	Cu_6Sn_5	Eutectic
C	Sn	Ag_3Sn	Eutectic
D	Ag_3Sn	Sn	Eutectic
E	Ag_3Sn	Cu_6Sn_5	Eutectic
F	Cu_6Sn_5	Ag_3Sn	Eutectic

Figure 5.1 Mapping of the 1st and 2nd phase field for various SAC alloys and Solidification sequence as a function of Ag and Cu composition.
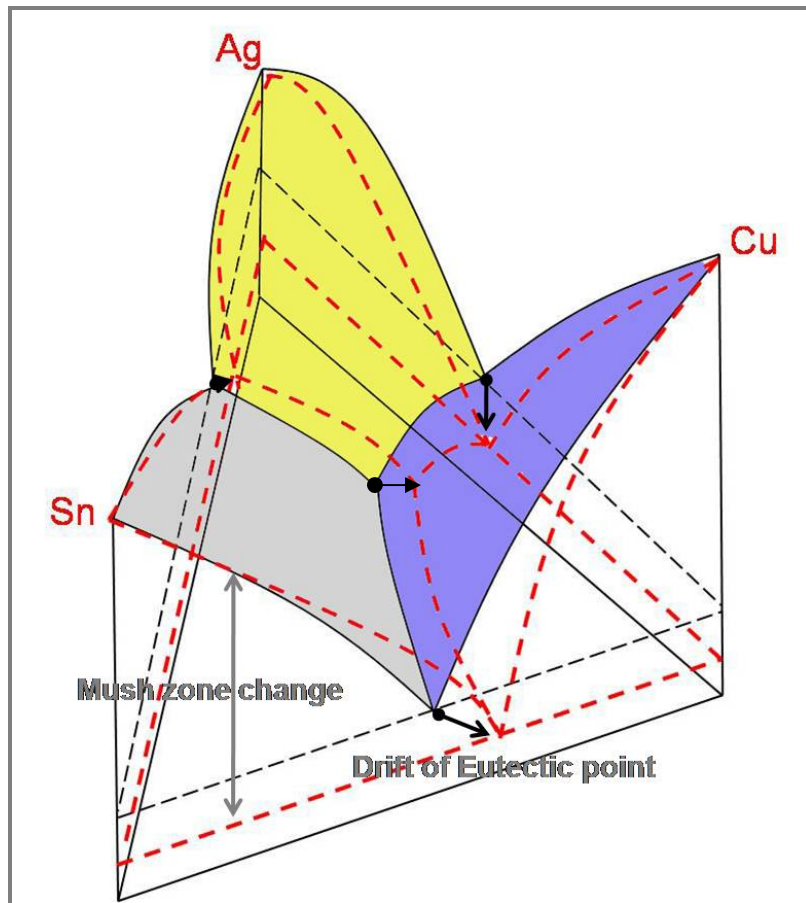
56

Figure 5.2 non-equilibrium phase diagram transformed by super-cooling.

5.3 Mechanism of Cu$_6$Sn$_5$ IMC Growth in Solder

The growth of IMC at Cu or NI pad has been extensively investigated; however, study on IMC within solder matrix has been limited. The growth of IMC phase or phases in solder matrix is usually ignored; probably due to more critical role that interfacial IMC is playing. However, present study finds that the IMC phase in the solder matrix also evolves significantly with aging. It is therefore anticipated that mechanical properties of solder is greatly affected by presence and evolution of IMC phases in solder matrix. In particular, Cu IMC (Cu$_6$Sn$_5$) is found to be important because it grows with unlimited supply of Cu from Cu pad.

As presented in the results, Cu IMC continues to grow with aging. If it is pure coarsening of existing Cu IMCs, their total volume fraction is supposed to remain constant. The fact that it increases with time, more at solder near Cu pad side, indicates that Cu IMC grows with the supply of Cu from Cu pad. The growth at Ni side is slow or absent by two possible reasons. The first is that majority of Cu entered solder from Cu pad is consumed by growing Cu IMCs at Cu pad side, resulting no or insignificant amount of Cu to reach Cu IMCs at Ni pad side. Alternatively, Cu can be drained away by NI side IMC. Ni is a diffusion barrier that prevents diffusion of Cu from underlying Cu, yet it forms Cu bearing NI-Sn IMCs. This reaction may drain Cu from nearby solder matrix. Figure 5.3 presents schematics of these two mechanisms. Currently, it is not clear which is predominant. Evidence exists that the latter may be the case. More investigation is needed for better understanding of proper mechanism responsible for slow growth in Ni side Cu IMCs.

Another area that needs more investigation is the mechanism of Cu entrance to solder matrix. Although it is usually referred to be a result of diffusion, it is not clear exactly how Cu enters Cu matrix. It is true that Cu enters solder by diffusion, but since Cu IMC growth also occurs at Cu interface the exact process is not as clear. The diffusion of Cu into solder matrix must occur at Cu$_6$Sn$_5$ IMC at Cu interface, meaning that it retards the growth of interfacial IMC. If out-flux from interfacial IMC into solder is greater than in-flux from Cu to Cu IMC, the Cu IMC

58

solder matrix can grow but interface IMC needs to shrink. On the other hand, if out-flux is less than the influx, interfacial Cu IMC can grow, but matrix IMC cannot grow with the same rate of interfacial IMC. This seems to be case. When matrix Cu IMC growth rate is compared with the growth rate of interfacial IMC, it is found that the former is far slower than the latter.
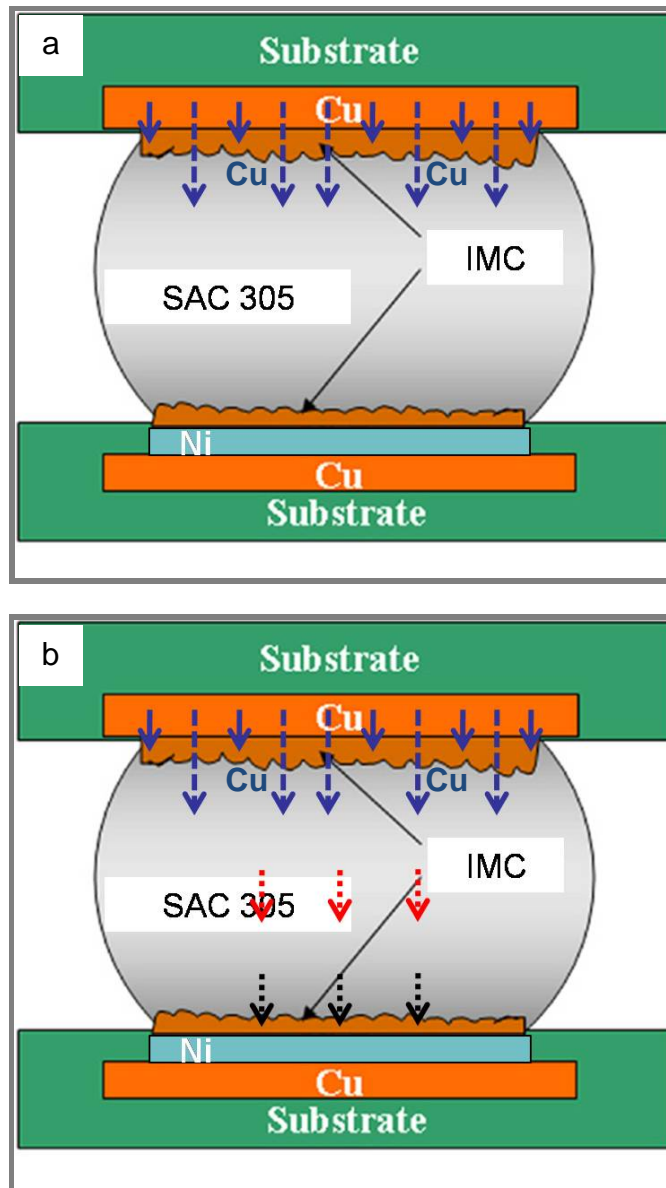

Figure 5.3 Schematic: two mechanisms showing the invariant volume fraction of Cu_6Sn_5 on Ni side matrix

CHAPTER 6

CONCLUSIONS

This study investigates the microstructural characteristics of SAC 305 solder assembly at as-reflowed and aged condition. The specific aging condition used is 100°C and 150°C for duration of 100, 200, 500, 1000hrs. The main foci of microstructural study is solder matrix (dendrite structure, eutectic, inner matrix IMC) and interfacial IMCs. The change in these microstructural features with aging is closely tracked by conducting optical microscopy, X-ray mapping and SEM inspection. From these investigations, the present study successfully makes following conclusions:

1) The composition of SAC 305 solder at as-reflowed condition is not the same as the bulk. It is found that the alloy is enriched with Cu by reaction with Cu pad. This, Cu enrichment, pushes the composition to the different phase field to yield solidification sequence of Cu_6Sn_5 as first primary phase, β-Sn as second primary phase. This solidification sequence is not possible without Cu enrichment.

2) It is found that the SAC305 solder joint develops highly non-equilibrium microstructure. It is found that the microstructure contains b-dendrite with a fraction far greater than the expected and also $Sn-Ag_3Sn$ eutectic rather than ternary eutectic. With large supercooling capability of Sn liquid, the eutectic temperature is believed to be pushed down to lower temperature than the equilibrium. This extends the Sn dendrite growth phase field, and the excessive growth is believed to consume Cu in the alloy. Hence,

60

the final liquid that is supposed to be ternary eutectic ends up with binary eutectic consisting of Ag_3Sn and Sn.

3) Aging is found to promote breakage of Sn-dendrite as a part of process restoring chemical equilibrium. With aging progresses, the β-Sn dendrite disappears and is growing to one grain.

4) Aging makes the eutectic phases to coarsen. However, since the starting eutectic is the binary eutectic, coarsening of only two phases (Ag_3Sn and Sn) is found to occur. Cu-rich phase present at eutectic pool boundary as-reflowed condition disappears with aging, probably as a part of homogenization of dendrite Sn.

5) It is found that Cu continuously enters solder matrix from Cu pad side with aging. With this, the inner Cu IMC is found to increase in size and volume fraction. However, the growth is found to be small or absent in the case of solder near at Ni matrix, probably due to small amount of Cu available for IMC growth.

REFERENCES

[1] Moore, G.E., "Cramming More components onto Integrated Circuits," Electronics, 1965, Vol. 38(8), p. 114-117.

[2] Tummala, R.R., Rymazewski, E.J., and Klopfenstein A.G., eds. Microelectronics Packaging Handbook. 2 ed. 1998, Kluwer Academic Pub.

[3] Brown, W.D., ed. Advanced Electronic Packaging with Emphasis on Multichip Modules. Ed. W.D. Brown. 1998, IEEE Press: New York.

[4] R. Tummala, E. J. Rymaszewski, and A. C. Klopfenstien, "Microelectronic Packaging Handbook - Semiconductor Packaging," Second ed. vol. 2: Chapman & Hill, 1997.

[5] NCMS, "Lead-free Solder Final Report, www.ncms.org," 1997.

[6] NEMI, "National Electronics Manufacturing Initiative, News Release," in www.nemi.org/PbFreePUBLIC/index.html, 2007.

[7] JEIDA, "Challenges and Efforts Toward Commercialization of Lead-free Solder - Road Map 2000 for Commercialization of Lead-free Solder," Japan Electronic Industry Development Association 2000.

[8] M. Abtew and G. Selvaduray, "Lead-free Solders in Microelectronics," Materials Science and Engineering, vol. 27, pp. 95-141, 2000.

[9] R. Darveaux and K. Banerji, "Constitutive Relations for Tin-Based Solder Joints," IEEE Transactions on Components, Packaging, and Manufacturing Technology, vol. 15, pp. 1013-1024, 1992.

[10] A. LaLonde, D. Emelander, J. Jeannette, C. Larson, W. Rietz, D. Swenson, and D. W. Henderson, "Quantitative Metallography of -Sn Dendrites in Sn3.8Ag0.7Cu Ball Grid Array

[11] Solder Balls via Electron Backscatter Diffraction and Polarized Light Microscopy," Journal of Electronic Materials, vol. 33, 2004.

[12] J. A. Rayne and B. S. Chandrasekhar, "Elastic Constants of Tin from 4.2°K to 300°K " Physical Review, vol. 120, pp. 1658-1663, 1960.

[13] B. Chalmers, "Micro-Plasticity in Crystals of Tin " Proceedings of the Royal Society of London, Series A, Mathematical and Physical Sciences, vol. 156, pp. 427-443, 1936. 158

[14] D. Frear and H. Morgon, in The Mechanics of Solder Alloy Interconnects, J. H. Lau, Ed., 1994.

[15] S. Weise, E. Meusel, and K. J. Wolter, "Microstructural Dependence of Constitutive Properties of Eutectic and SnAg and SnAgCu Solder," in Proceedings of 53rd Electronic Components and Technology Conference, New Orleans, 2003, pp. 197-206

[16] L. T. Yeh, "Review of Heat Transfer Technologies in Electronic Equipment", Journal of Electronic Packaging, Vol. 117, pp. 333-339, December 1995.

[17] Abtew, M., Selvaduray, G., "Lead-Free Solders in Microelectronics," Materials Science and Engineering, Vol. 27, 2000, pp. 95-141.

[18] Karlya, Y., Gagg, C., Plumbridge, W. J., "The Tin Pest in Lead-free Solders," Soldering and surface Mount Technology, Vol. 13, pp. 39-40, 2000.

[19] Karlya, Y., Gagg, C., Plumbridge, W. J., "The Tin Pest in Lead-free Solders," Soldering and surface Mount Technology, Vol. 13, pp. 39-40, 2000.

[20] Lee, N. C., "Getting Ready for Lead-free Solders," Soldering & Surface Mount Technology, Vol. 26, pp.65-74, 1997.

[21] Soldertec, European Lead-free Roadmap, Ver.1, pp. 1-26, 2002.

[22] Nimmo, K., "Alloy Selection," Chapter 3 of Lead-free Soldering in Electronics: Science, Technology and Environmental Impact, edited by K. Suganuma, New York, Marcel Dekker, pp. 61-62, 2004.

[23] http://www.tulane.edu/~sanelson/geol212/ternaryphdiag.htm.

[24] http://www.metallurgy.nist.gov/phase/solder/solder.html.

[25] Ye, L., Lai, Z. H., Liu, J., Thölén, A., " Microstructure Investigation of Sn-0.5Cu-3.5Ag and Sn-3.5Ag-0.5Cu-0.5B Lead-free Solders," Soldering & Surface Mount Technology, Vol. 13, pp. 16-20, 2001.

[26] Iting, T., Li, J. T., Yen, S. F., Chuang, T. H., Lo, R., Ku, T., Wu, E., "Identification of Mechanical Properties of Intermetallic Compounds on Lead Free Solder," Proceedings of the 55th Electronic Components and Technology Conference, pp. 687-691, 2005.

[27] Fields, R. J., Low, S. R., "Physical and Mechanical Properties of Intermetallic Compounds Commonly Found in Solder Joints," available online at:

http://www.metallurgy.nist.gov/mechanical_properties/solder_paper.html.

[28] Ganesan, S., Pecht, M., Lead-free Electronics, Wiley-Interscience Publication, pp.51-52, 2006.

[29] Hwang, J., Environment-Friendly Electronics: Lead Free Technology, Electrochemical Publications, pp. 134-137, 2001.

[30] Reed, J., "Immersion Silver as a Replacement for Solder Finish" IPC/SMTA Electronics Assembly Expo, Providence, RI, 1998, pp. S23-3-S23-3-11

[31] Lau, J., "Ball Grid Array Technology", McGraw-Hill, New York, 1995.

[32] Stafstrom, E., "Unraveling the Final Finishing Mystery", Circuits Assembly,November 2000, pp, 56-62.

[33] Whiteman, L., "Issues and Solutions to Implementing Lead-Free Soldering", Journal of Surface Mount Technology, Vol. 13, No. 4, October 2000, pp, 15-22.

[34] Mei,Z., "A Failure analysis and rework method Electronic Assembly with Electroless Ni/Immersion Au Surface Finish", Proceedings - SMTA International, Chicago, IL, September 1999, pp, 407- 411

[35] Huang, X., Lee, S. Yan, C.C., Hui, S., "Characterzation and Analysis on the solder Ball Shear Testing Conditions", Proceedings - Electronics Components and Technology Conference, Orlando, FL, 2001, pp, 1071-1075

[36] L. P. Lehman, R. K. Kinyanjui, L. Zavalij, A. Zribi, and E. J. Cotts, "Growth and Selection of Intermetallic Species in Sn-Ag-Cu No-Pb Solder Systems based on Pad Metallurgies and Thermal Histories," Electronic Components and TechnologyConference, pp. 1215-1221, 2003.

[37] L. P. Lehman, S. N. Athavale, T. M. Fullem, A. C. Giamis, R. K. Kinyanjui, M. Lowenstein, K. Mather, R. Pater, D. Rae, J. Wang, Y. Xing, L. Zavalij, P. Borgesan, and E. J. Cotts, "Growth of Sn and Intermetallic Compounds in Sn-Ag-Cu Solder," Journal of Electronic Materials, vol. 33, pp. 1429-1439, 2004.

[38] L. Snugovsky, P. Snugovsky, D. D. Perovic, T. Sack, and J. W. Rutter, "Some Aspects of Nucleation and Growth in Pbfree Sn-Ag-Cu Solder," materials Science and Technology, vol. 21, pp. 53-60, 2005.

[39] A. W. Gibson, S. L. Choi, K. N. Subramanian, and T. R. Bieler, "Issues Regarding Microstructural Coarsening Due to Aging of Eutectic Tin-Silver Solder," in Reliability of Solders and Solder Joints, TMS, R. K. E. Mahidhara, Ed., 1997, p. 97.

[40] P. L. Tu, Y. C. Chan, K. C. Hung, and J. K. L. Lai, "Growth Kinetics of Intermetallic Compounds in Chip Scale Package Solder Joint," Scripta Materialia, vol. 44, pp. 317-323, 2001.

[41] L. Qi, J. Huang, J. Zhang, and Y. Wang, "Microstructure and Intermetallic Growth at the Sn-Ag-Cu/Ni Interface after Thermal-shearing Cycling," 6th International Conference on Electronic Packaging Technology, pp. 720-723, Sept 2005 2005.

[42] P. Arulvanan, Z. Zhong, and X. Shi, "Effects of Process Conditions on Reliability Microstructure Evolution and Failure Modes of SnAgCu Solder Joints," Microelectronics Reliability, vol. 46, pp. 432-439, 2006.

65

[43] E. Bradley, C. Handwerker, J.E. Sohn, Surf. Mount Technol. (SMT) 17 (2003) 1.

BIOGRAPHICAL INFORMATION

He began his academic career in 1998 at Changwon National University in changwon, KOREA. After military service period (2000.01~20004.04), the field of Material Science and Engineering quickly fascinated his attention as a future career. As a senior, he did research in the area of manufacturing conventional metal; stainless steel, carbon steel, etc. This research sparked his interest in solidification and foundry process. After graduation from undergraduate school, he settled at the solidification lab in Changwon National University as in master course. He had researched the field of solidification behavior and investment casting of commercial metal including superalloy and taken part in several projects to develop advanced components and equipment for around 2 years. During that period, he desired to study abroad. Finally, he got the chance to do it under the co-degree program and left to Texas, America in Jan. 2009. The University of Texas at Arlington welcomed him into the family with open arms to pursue a master's degree in materials science and engineering. With the opportunity to enter the arena of electronic materials, he chose to work in the area of lead-free solders. Under the guidance of Dr. Choong-Un Kim, he studied electronic materials and performed the project with Cisco system Co. Eventually, he graduate from UTA after only a year since he entered in UTA. His future plans include becoming a CEO and contributing to society as a philanthropist.